

# Use of Multiscale Entropy to Characterize Fetal Autonomic Development

By

© 2019

Kimia Memar

B.Sc., Southern Illinois University, 2015

Submitted to the graduate degree program in Bioengineering and the Graduate Faculty of the University of Kansas in partial fulfillment of the requirements for the degree of Master of Science.

---

Chair: Dr. Jonathan Brumberg

---

Co-chair: Dr. Kathleen Gustafson

---

Member: Dr. Glenn Prescott

Date Defended: 9 April 2019

The thesis committee for Kimia Memar certifies that this is the  
approved version of the following thesis:

## Use of Multiscale Entropy to Characterize Fetal Autonomic Development

---

Chair: Dr. Jonathan Brumberg

---

Co-chair: Dr. Kathleen Gustafson

Date Approved: 9 April 2019

## Abstract

The idea that uterine environment and adverse events during fetal development could increase the chances of the diseases in adulthood was first published by David Barker in 1998. Since then, investigators have been employing several methods and methodologies for studying and characterizing the ontological development of the fetus, e.g., fetal movement, growth and cardiac metrics. Even with most recent and developed methods such as fetal magnetocardiography (fMCG), investigators are continuously challenged to study fetal development; the fetus is inaccessible. Finding metrics that realize the full capacity of characterizing fetal ontological development remains a technological challenge. In this thesis, the use and value of multiscale entropy to characterize fetal maturation across third trimester of gestation is studied. Using multiscale entropy obtained from participants of a clinical trial, we show that MSE can characterize increasing complexity due to maturation in the fetus, and can distinguish a growing and developing fetal system from a mature system where loss of irregularity is due to compromised complexity from increasing physiologic load. MSE scales add a nonlinear metric that seems to accurately reflect the ontological development of the fetus and hold promise for future use to investigate the effects of maternal stress, intrauterine growth restriction, or predict risk for sudden infant death syndrome.

## Acknowledgements

I live a hemisphere away from my family, and they endure this, so I could pursue my dreams. I want to thank them for their infinite love and never-ending kindness. My mother's pursuit of her education and a career encouraged me to do the same.

I would like to thank my husband, Reza Ahmadi, for his unconditional love and persistent support, inspiring me to set no limits on my ambitions and never give up or stop growing.

Also, I want to thank my adviser, Dr. Kathleen Gustafson and her team at Hoglund Brain Imaging Center for making my graduate studies possible. Being part of her team, I discovered my passion for science, not only as the road to the truth, but also as a way of life.

## Table of Contents

Chapter 1: Introduction.....	1
Clinical Fetal Monitoring .....	2
Fetal Research.....	2
Methods for Fetal Developmental Assessment .....	3
Chapter 2: Literature Review.....	9
Fetal Research.....	9
Fetal Heart Rate and Heart Rate Variability.....	10
FHR and FHRV Monitoring Methods.....	13
Fetal Magnetocardiography (fMCG).....	15
Chapter 3: Materials and Methods.....	17
fMCG Recording.....	17
EEGLAB .....	18
fMCG and EEGLAB .....	19
KubiosHRV .....	20
Data Collection .....	22
Edit Preferences.....	25
Analysis Options.....	26
Report Settings .....	27

Specific Preference Settings for This Thesis .....	28
Artifact Correction.....	31
Samples for Analysis.....	32
Remove Trend Components .....	32
The Data Browser Segment.....	33
The Results View Segment.....	33
Time Domain.....	34
Frequency Domain .....	34
Nonlinear .....	35
Time-varying results.....	35
Our processing.....	36
HRV Metrics and Methodologies .....	37
Time domain.....	38
Frequency Domain .....	40
Nonlinear Methods .....	42
ApEn.....	42
SampEn.....	44
Multiscale Entropy .....	48
Poincare Plot.....	52

Stress Index And PNS/SNS Indexes .....	53
Chapter 4: Results.....	56
Chapter 5: Discussion .....	62
References.....	66

## List of Figures

Figure 1. Electrophysiology of the Heart [35] .....	12
Figure 2. 83 Channel Investigational Biomagnetometer .....	17
Figure 3. Component activities, EEGLAB .....	24
Figure 4. Time-domain, frequency-domain, and nonlinear analysis results in Kubios report.....	36
Figure 5. Time-Varying results in Kubios report.....	37
Figure 6. HR time series and RR series example.....	39
Figure 7. Frequency domain spectrum example.....	41
Figure 8. Course-Graining Procedure [52] .....	50
Figure 9. PNS and SNS index.....	55
Figure 10. Poincare Plot - subject 1 .....	57
Figure 11. Poincare Plot, subject 2 .....	57
Figure 12. Scale 1 to 20 MSE for subject 1 (high PNS) and subject two (low PNS).....	58
Figure 13. Median split of sample entropy (MSE 1) in two groups of 71 individuals each.....	59
Figure 14. Scale 1 to 20 average MSE for 43 fetal subjects - 32 wks and 36 wks .....	60
Figure 15. Scale 1 to 20 average MSE for 33 maternal subjects - 32 wks and 36 wks .....	61





## List of Tables

Table 1. Input Data and Pre-processing Settings.....	28
Table 2. Analysis Options Settings.....	29
Table 3. Time/Frequency Domain Settings .....	29
Table 4. Nonlinear Settings .....	30
Table 5. Time – Varying Settings.....	30
Table 6. Fetal and Maternal Average Sample Entropy.....	56
Table 7. mean and SD of multiscale entropies of subjects in figure 13- The mean and SD MSE scales 2-20 of 142 pregnant women are shown in table 2. A median split of the 142 samples allowed the classification of two groups; low and high sample entropy. ....	59

## Chapter 1: Introduction

*“The Womb May Be More Important Than The Home,”* David J. P. Barker, 1990 [1]

In 1990, with the emergence of studies on relationships between early life placental and birth weight and later life risk of hypertension, and through several similar epidemiological findings, Barker [1] began to explore the link between fetal and infant growth and adult cardiovascular disease. He started shaping his hypothesis about the significance of long term programming in early life. Using the new knowledge of fetal processes that could determine programming, he focused on developing a new model of adult degenerative diseases which would involve programming by the environment in fetal and infant life.

In 1998 Barker [2] published the “Barker hypothesis,” stating that factors during critical periods of gestation predispose the fetus to certain postnatal diseases. That is, disruption or adverse stimuli at critical times of embryonic and fetal development can lead to developmental adaptations with changes through structural, physiological and metabolic mechanisms which could predispose the individual to metabolic, cardiovascular or endocrine diseases in adult life; now termed developmental origins of health and disease (DOHaD).

After Barker’s seminal publication, a PubMed search shows over 4000 publications related to fetal programming in human and animal models. More than 300 of these publications are directly measuring effects of fetal programming. Research on animal models has been more informative with respect to mechanisms, largely due to more invasive outcomes measures [3]. However, research on human fetal programming has mainly used birth weight as the most readily available measure of fetal growth which is what Barker used more than 20 years ago. Both low and high birth weights could put the fetus at greater risk for obesity and metabolic diseases later in adult life

[4] [5] [6] . Also, research would benefit from measures more specific to understanding the neurodevelopment of the fetus. With ever increasing evidence of developmental programming effects and expanding needs for understanding its mechanisms, the field of human fetal programming is in need of methodologies and metrics that accurately and realistically index fetal programming and explain its mechanisms [7].

### **Clinical Fetal Monitoring**

Clinicians typically monitor fetal well-being throughout gestation with measures of growth, observational nonstress tests (fetal body and breathing movements), heart rate, and during delivery, heart rate patterns. Doppler ultrasound is routinely performed to evaluate the intrauterine environment, e.g., amniotic fluid sufficiency, vascularity of the umbilical cord, or to check for structural malformations of the fetus. Cardiography is used during parturition to ensure fetal well-being and evaluate its readiness and survival during labor. The biophysical profile is a more integrative test which includes electronic fetal monitoring and fetal breathing motions, motor tone and amniotic fluid adequacy. These methods, while useful for monitoring the well-being of the fetus, are too insensitive and nonspecific to be useful for developmental research [8].

### **Fetal Research**

Characterizing Fetal Development – Distinct fetal HR patterns are well-known and linked with specific fetal activity states. These states are quiet sleep (1F), active sleep (2F), quiet wakefulness (3F) and active wakefulness (4F) [9] . These behavioral patterns have been studied by combining ultrasonic observations and the above methods to monitor fetal heart rate. Even though this gives information about fetal behavior towards evaluating fetal well-being or detecting a compromised fetus, it gives little insight to distinguish between normal and deviant

neurodevelopment. Therefore, while this is useful for clinicians and during delivery monitoring, it is not informative for understanding the ontological development of the fetus and is not sensitive enough to study potential fetal programming effects [10].

### **Methods for Fetal Developmental Assessment**

Fetal developmental programming investigators have recognized the need for improved measures to estimate the ontological development of the fetus. Therefore, several experts focused on defining better methods. They looked at several aspects of the fetus such as behavior, movement, brain development and the extent of its relationship to maternal factors. DiPietro et. al., conducted eight longitudinal studies of maternal fetal pair from June 1997 to February 2013, referred to as the John Hopkins Fetal Neurobehavioral Project. They collected data through a combination of brief ultrasound scans and the method of fetal actocardiography. Fetal actocardiography is based on a subset of electronic fetal monitors which can extract fetal motor activity from Doppler signals through a single wide array transabdominal Doppler transducer which also detects fetal heart rate. Fetal actocardiography detects fetal movements by bandpassing signals with the highest and the lowest frequency and maintaining the remaining signal [8].

In attempts to characterize the self-organization, adaptation and the individual development of the fetus, DiPietro explored heart rate movement coupling and found evidence that individual differences in HRV originate before birth and persist from prenatal to postnatal life. She observed correlations between fetal movement and HR accelerations which were especially evident in the third trimester and could be related to central nervous system maturation. In addition to findings about possible coordination of autonomic and motor function, DiPietro studied the effects of mild to moderate prenatal stress on motor development and association between the mother's emotional state and the behavior (heart rate of) her fetus in later pregnancy [11]. For example, she and

colleagues saw that the attitude of the mother towards pregnancy influences the level of motor activity in the fetus [12] .

DiPietro's efforts, among others established the association of maternal stress and anxiety with ultrasonographically observed fetal behavior and fetal heart rate [12], but she herself recognizes the limitations of Doppler Ultrasound. Even though this was the only commercially available means for both clinical and research use for a long time, it does not have the capacity for generating true interbeat (IBI) intervals and therefore has very limited use in developmental psychophysiological research [8].

Other researchers advanced the field by recognizing the limitations of standardized time- and frequency-domain HRV metrics for use in the fetus and realized the influence of fetal activity states and other typical movements on fetal HRV [13] . David et al., analyzed fetal HRV using a continuous wavelet transform and observed differences in fetal HRV across time and frequency [14] . They established specific frequency bands for the fetus that differ from adults, given the higher HR and other significant differences between adults vs. the fetus.

They used fetal and maternal ECG signals recorded by a FECCG and heart rate monitor system. ECG has several complications such as electrical interference from external sources or maternal abdominal muscle activity, and attenuation of the intensity of fetal R-waves due to the electrical isolation created by fetal vernix. In spite of that, they were able to detect beat-to-beat fetal R waves accurately enough to use is for exploring fetal autonomic development and maturation [14]. In addition, they have appreciated more than other investigators at the time, noting the challenges and limitations of standard HRV metrics in spite of their clinical application, and the challenges of studying the fetus, an organism in a fluid environment, who is not breathing and yet has periodic

diaphragm movements, and whose HRV changes with changing activity states, different neurobehaviors, and maturation.

Fetal magnetocardiography (fMCG) is an approach for noninvasive detection and recording of the fetal magnetocardiogram. Magnetic fields are generated by electric currents in the maternal and fetal bodies [15]. Using fMCG, Wakai showed that short-term and long-term fetal heart rate variability (fHRV) change during gestation and this may suggest the differential maturation of processes that control fHRV. He focused on fetal arrhythmias and observed an increase in fetal breathing movements and RSA in the third trimester of pregnancy [16]. Wakai also made efforts to characterize the influence of fetal state on heart rate variability [17].

Van Leeuwen and Cysarz et. al., looked at maternal– fetal HR interaction and synchronization [18] . Based on the observations that fetal heart rate changes with changes in physiological and psychological state of the mother and therefore correlated behavior of mean heart rates of mother and the fetus, and suspecting a specific coupling between maternal and fetal cardiac systems, they [19] found a phase synchronization between heartbeats of mother and fetus. In their work, they used multichannel magnetocardiography which simultaneously recorded the magnetic fields generated during each maternal fetal heartbeat at resting supine state [20]. Hoyer et. al., proposed a fetal autonomic brain age score using fetal heart rate patterns which he composed by time and frequency domain indices computed from fetal diagrams [21].

As methods such as Doppler US and fMCG were explored further by these researchers and when they were sufficiently developed, Gustafson et al., used fetal biomagnetometry to characterize specific fetal neurobehaviors and their corresponding magnetic field properties as well as their effect on cardiac autonomic control. They characterized fetal neurobehaviors such as non-nutritive suck (NNS), hiccups, and breathing movements and showed how the fetus modulates

heart rate around these behaviors [7, 22-24]. Their work advanced fetal developmental research from crude assessments towards using these methods, by primarily testing whether metrics of fetal HRV were sensitive enough to detect differences in groups where maternal factors might influence the development of cardiac autonomic control [25] .

Gustafson explored the roles of several interventions on the development of fetal neurobehaviors and autonomic control. One of these studies investigated the effect of maternal physical activity on fetal and infant cardiac autonomic control. The investigators showed that maternal physical activity can influence development of fetal cardiac autonomic control and the duration and intensity of exercise is a determining factor of this influence. They also found that these effects carry on into the infant period and concluded that maternal exercise has a programming effect on offspring cardiac autonomic control rather than a transient in-utero phenomenon [25, 26] .

Maternal-fetal biomagnetometry was used in a randomized clinical trial designed to determine the effect of docosahexaenoic acid (DHA), supplements taken by pregnant participants throughout the last two trimesters of pregnancy, on fetal autonomic development [7]. The results of this study showed that DHA supplementation to the mother increases fetal HRV [27] . It also led to evidence that suggested this effect was global and extended to both branches of the ANS rather than just specific to one. This was further validated by two Neonatal Behavioral Assessment Scale (NBAS) clusters turning out significantly higher in babies whose mothers received DHA, which signifies improved function in specific neurobehavioral domains [7, 28].

Fetal biomagnetometry, or fetal magnetocardiography (fMCG) is much more precise and reliable than other methods and it is noninvasive. fMCG is very sensitive to the changes in coordination and orientation of the fetal heart [7, 8]. Even though fetal biomagnetometry shows



great promise as a noninvasive and sensitive method for understanding the effects of interventions on physiology and neural integration, the limitations of HRV analysis in the fetus are still recognized. In adults, HRV are used in clinical assessment of cardiac health. HRV metrics have extended to psychological research to study vagal influence [29]. In the fetus, HRV has been used as proxy for central and peripheral nervous systems assessment and the degree of integration and coupling between them at different points during development. Therefore, there is a need to discover better methods and metrics which fully realize the capacity of HRV in measuring and understanding this integration between multiple systems in control of neurodevelopment and therefore development overall [7].

For the field of fetal developmental research to advance, there is critical need for more sensitive and integrative measures that can inform the developmental processes and mechanisms that reflect maturation and integration of the fetal nervous system. The aim of this thesis is therefore to explore nonlinear metrics of HRV to evaluate whether these metrics better model the development of the fetus. Specifically, to find whether nonlinear metrics of entropy can characterize the autonomic integration during fetal development throughout gestation. [having in mind that the increase in maternal HR and decrease in maternal HRV with pregnancy has been established [30], and to better distinguish the role of entropy in reflecting development, we compare and contrast the way entropy represents fetal HRV changes with maternal HRV changes during gestation.

We predict that as the fetus develops, the increased influence of vagal control will be reflected in the trends of Multiscale entropy, which is a nonlinear measure of HRV. As the fetus progresses past 30 weeks of gestation, changes in activity states and brain maturation occur which are

attributed to increased vagal control [8]. If our hypothesis is true, we should see increased vagal influence apparent in MSE scales between 32 and 36 weeks.

## Chapter 2: Literature Review

### Fetal Research

Fetal surveillance based on cardiac signals has been in place since 1600 [31] and more widely spreading around 1940s. Around 1980s when scientists became particularly interested in fetal development and research, heart rate as a way to assess well-being by clinicians increased; several tools towards reliably recording Fetal Heart rate (FHR) were created. Since then, documentation of fetal development using new devices and methods for FHR monitoring and interpretation became prominent [8]. There were many reasons for the increased focus on FHR, along with new devices and methods for FHR monitoring and interpretation, which started then and is continuing nowadays. Firstly, studies showed characteristic changes to HR patterns correlated with general placental under-perfusion and hypoxic events. Secondly, FHR is the most available and direct measure for monitoring fetal breathing, and thirdly, it is a way to assess fetal behavior [8, 16].

From a clinical standpoint, fetal health has been connected to fetal breathing, fetal movement and overall fetal behavior. This was due to observations that a fetus with a compromised health for any reason, shows limited physical mobility. Characterization of fetal behavior is the basis of neurodevelopment. On the other hand, the heart is largely under the influence of the autonomic nervous system. The SA node which on its own would lead the heart to beat at a constant rate, the conduction system and the myocardium are innervated by the ANS nerves. Sympathetic and Parasympathetic nervous system, two branches of ANS, work antagonistically and their constant activity is mediated by the Autonomic Nervous System. FHR is therefore the most tangible tool for understanding, monitoring and potentially improving fetal neurodevelopment and ultimately prenatal and neonatal health [8, 16]. Today clinical FHR measurement and monitoring is performed in clinic for ensuring fetal health throughout gestation and adequate oxygenation during

delivery. In research it is of interest for understanding fetal behavioral and neurodevelopmental processes and creating early diagnostic methods [31] .

### **Fetal Heart Rate and Heart Rate Variability**

As early as the 1900, investigators looked at HR and HRV and noticed how they change with developmental advances and asked questions about the specific sources of these changes [32]. FHR was then and is now still an available measure of monitoring and assessing the fetus. The first tool for FHR measurement was a stethoscope used on the pregnant mother's belly and since then different tools have been developed which are mostly based on principles such as Doppler ultrasound, bioelectric fetal signals and electromagnetic fetal signals.

The simplest and oldest use of FHR was for ensuring general fetal wellbeing throughout pregnancy and during labor. Several tests and procedures have been carried out and various new protocols have been developed to respond to evolving clinical practices over time. Beginning nearly 40 years ago, non-stress testing of the fetus was incorporated into prenatal care protocols. This test was the first evaluation method which acknowledged and emphasized the connection between FHR accelerations and fetal health [33] . The fetal non stress test is the current primary clinical tool for externally monitoring the fetus, looking for fetal heart rate variability, specifically FHR accelerations due to fetal movements and other uterine activity [34]. This is a general and non-sophisticated test which categorizes the fetus as non-reactive if it detects less than two accelerations of 15 bpm or greater in 20 minutes [8, 33] . For adults, HRV is studied in the areas of cardiovascular disease, renal failure, smoking and drug addiction, sports, anxiety and depression. Some specific clinical uses are in predicting sudden cardiac death after acute myocardial infraction or diabetic cardiovascular autonomic neuropathy [35] . Some of the most recent clinical uses of FHR is in understanding the process of neurodevelopment and early and

noninvasive diagnosis of related pathologies, as well as fetal network physiology and the mechanism which engineers the coupling of fetal and maternal systems.

Heart rate variability (HRV) by definition is the variations between consecutive inter-beat-intervals (IBIs), or changes in heartbeat interval and is in a way, reciprocal of the HR. HR is controlled and regulated by the ANS through its connections with the CNS called Central Autonomic Network. The sympathetic (SNS) and parasympathetic (PNS) branches of the ANS have different influences on HR. SNS activity increases HR and decreases HRV, while PNS actions lead to decreased HR and increased HRV. In addition to this central influence, quick changes in HR occur by the arterial baroreceptor reflex which affects the sympathetic and parasympathetic activity and respiration [35] .

For the fetus, these controls can be divided into the two categories of neural and non-neural regulation. Neural control which is driven by SNS and PNS changes throughout gestation. AS the parasympathetic and sympathetic innervations progress, the parasympathetic influence increases and the role of autonomic control which is initially performed by medulla oblongata is undertaken by higher cortical areas. Non-neural regulation is through physiological processes such as metabolic pathways [8, 16] . HRV is valuable because it gives information about these controlling pathways and systems such as nervous system inputs, adaptability and capacity of autonomic regulation and its balance, and status of developing systems within fetal body [8] , and physiological regulation.

As previously mentioned, HRV is very important to understanding the ANS. The autonomic control generates the sinus rhythm of the heart in the SA node. Tracking the action potentials in the SA node for HRV measurement is not practically possible. In an ECG, the closest event to the SA node firing is atrial depolarization which is observed as the p-wave in the QRS complex. The

time between the two P-waves is therefore the period of the heartbeat. However, Ventricular depolarization contributes much more to the QRS complex than atrial depolarization and causes a better signal to noise ratio when compared with P-wave. Therefore the time between two QRS complexes instead of that of the p-waves is the basis for computing the heart beat period [35]. The contribution of ventricular depolarization is shown in figure 1.

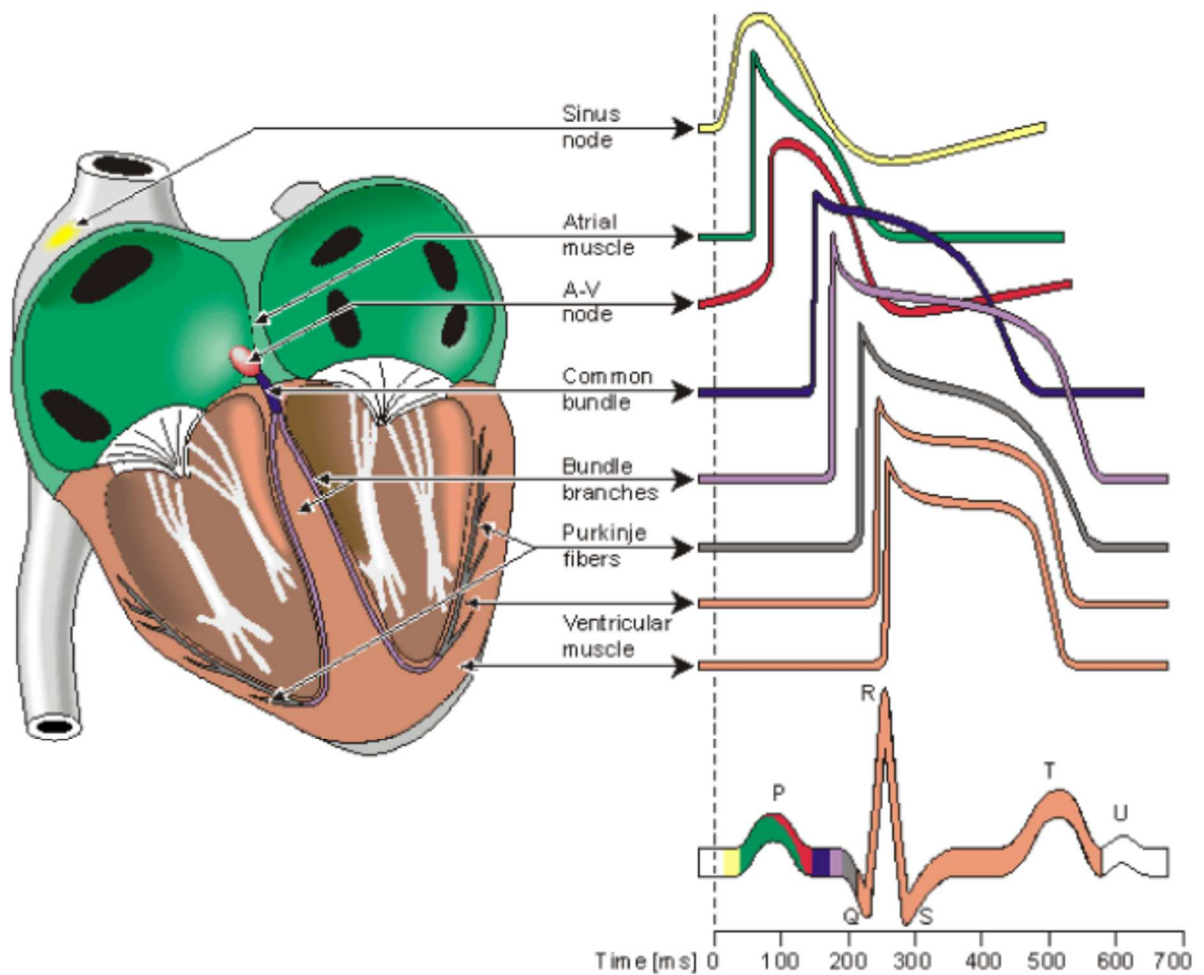


Figure 1. Electrophysiology of the Heart [35]

## **FHR and FHRV Monitoring Methods**

Some of the earliest fetal research involved auscultation; simply using a stethoscope to hear fetal heart beat through the mother's abdomen. The heart beats were manually timed using a stopwatch and then either averaged to estimate the mean heart rate or were plotted for limited time durations. Years later, electronic fetal monitors for automatic detection of FHR were devised. Also called fetal cardiography, this method detects motions of the fetal heart, and therefore fetal heart beats based on Doppler, by detecting the frequency changes resulting from each systole. Autocorrelation methods are then employed for quantifying FHR.

The majority of fetal monitoring studies so far have been conducted based on Doppler detected fetal heart rate as a commercially available and affordable technology for both research and clinical use [8]. Ultrasound imaging, offered in three types of B-mode, M-mode and Doppler ultrasound, is still a widely used technique by mainstream researchers. B-mode and M-mode ultrasound both rely on two-dimensional cross-section images of the fetus, but M-mode offers more accuracy and detail because of continuous scanning of cross sectional images and therefore improved temporal resolution and, simultaneous structural measurements and comparisons during the cardiac cycle. B-mode ultrasound is suitable for general structural information such as head circumference (HC) or femur length (FL). M-mode offers more heart-specific structural insights such as ventricular walls thicknesses or systolic/diastolic diameter, and interventricular septum thickness [15]. As mentioned above, Doppler ultrasound is used for the measurement of fetal heart rate, while also reporting on fetal circulation. As parts of tissues/organs such as heart walls move with respect to the ultrasound transducer, the resulted Doppler shifts are measured, ultimately enabling detection and tracking of fetal Respiratory Sinus Arrhythmias. Three dimensional (3D) color Doppler echocardiography and 4D fetal Doppler echocardiography are two recent extensions of Doppler

ultrasound which provide volumetric information about the fetal body and minimize the image reconstruction lag respectively and therefore present improved quantity and quality of information [15].

Doppler is indeed a valid method for quantifying FHR, but it lacks the capability to create true interbeat (IBI) intervals and therefore does not tell much about FHR variability which is highly required for any developmental fetal research. Also it is contaminated with artifacts and noise, hence requiring sophisticated signal processing techniques [15]. In recent years it became evident to physicians, scientists and researchers that unlike research of any other period of human life, fetal and prenatal science depends critically on technology and its capabilities in answering even the simplest questions. Focus of the research community partially shifted towards sophisticated imaging and HR measurement technologies after going back and forth between complicated unanswered questions [8]. A few other approaches have been developed for detecting the electrical or electromagnetic signals of the fetal R-wave noninvasively through the maternal abdomen surface [8]. Today, the most widely used techniques are ultrasound imaging, fetal electrocardiography (fECG) and fetal magnetocardiography (fMCG) [15].

fECG measures the heart's electrical activity and heart beat patterns. In spite of low cost and accessibility of this method, it has several disadvantages. It is very difficult to set apart electrical fetal signals from larger and stronger maternal signals through transducers which are placed on the maternal abdomen. This is a bigger problem early during gestation due to weak fetal cardiac readings as well as later during weeks 24 to 36 due to the relatively rapid thickening of vernix caseosa which is an electrical insulator [8, 15, 16].



## **Fetal Magnetocardiography (fMCG)**

fMCG was first performed in 1974 by A gradiometer type SQUID magnetometer intended to reach the sensitivity of 10 nGauss with a 100 Hz bandwidth, in a wooden cottage 70 m away from the nearest residential areas [36] . At first, many investigators used this approach to study congenital heart defects such as congenital atrioventricular block in fetuses [37] . Longitudinal research with MCG later developed and led the field towards more focus on growth and developmental questions. As the role of autonomic nervous system on fetal development and cardiac control was investigated by fMCG experts, more specific topics such as the influence of fetal states or other factors on HR and HRV [38] , fetal-maternal coupling and network physiology [39] , clinical diagnosis of serious fetal arrhythmia [40] and fetal brain age score [21] raised. What has been suggested by recent research is the individuality of HRV which is one of the most significant findings for the future of fetal development research [31] .

Known for its precision in assessment of fetal beat-to-beat HRV, fMCG is an approach for noninvasive detection and recording of fetal R-waves which records the magnetic fields generated by electric activities in the fetal/maternal body. This electrical activity could come from many sources such as the eye, the brain, the heart and any type of fetal movements such as trunk movements or breathing activity. The advantage of this over FECG is that magnetic signals do not suffer from low conductivity or contamination by noise and maternal signals as much as electric signals [15].

In general, biomagnetic and bioelectric signals have similar features and quality, but for fetal signals this is not the case. Fetal electric signals are weak with lots of interference from maternal signals and a low amplitude. Fetal magnetic signals are on the other hand offering notable higher quality even as early as 20 weeks gestation [16] .

fMCG is therefore much more reliable even though it is largely altered by the distance between sensors or between sensors and the source as well as the configuration of the volume conductor. This is different from person to person or depending on the gestational age [15]. fMCG is very sensitive to the changes in coordination and orientation of fetal heart and this was how fMCG actography developed. Fetal actocardiography bandpasses extreme frequency signals such as fetal heart rate signals with high and maternal somatic activity with low frequencies and maintains the remaining signal which is indicative of movements [8]. Fetal actography is a way of inspecting fetal activity. Fetal trunk movements are the most noticeable and important movements which result in episodic variations in signal baseline and amplitude [16]. fMCG is therefore very suitable for detecting and analyzing gross fetal trunk movements and general fetal activity [16].

Due to its accuracy, robustness, reliability and noninvasiveness, fMCG has been deemed as an appropriate approach for monitoring and understanding the effects of different factors such as nutrition on the development of fetus and the autonomic control of the heart [31]. Several findings of fMCG such as its detection of RSA have proven this method exceptionally useful and important in understanding and predicting important neonatal problems such as sudden infant death syndrome. This is just one example of how fMCG alone has revolutionized and increased the diagnostic and predictive value of FHR and FHRV [16].

## Chapter 3: Materials and Methods

### fMCG Recording

The first step of the study is recording fetal and maternal HR using an investigational biomagnetometer with 83 channels, shown in figure 2. This device is custom-designed by CTF systems (a subsidiary of VSM MedTech, Ltd) and placed in a magnetically shielded room to prevent noise and contamination from any other magnetic fields outside maternal body. The sensor array is distributed specifically to span across the gravid maternal abdomen. These sensors are particularly sensitive axial gradiometers that use superconducting quantum interference devices (SQUID) to detect even the weak magnetic fields coming from the inside of maternal body. The 83 channels enable simultaneous multichannel recordings and therefore a time resolution of millisecond. Fetal biomagnetometry is a preferred method for FHR and FHRV analysis because in addition to overall exceptional quality of recordings, it is completely noninvasive, it records biomagnetic signals from sources in addition to the heart, and it records the QRS complex and therefore precisely each R-peak which is necessary for accurate HRV measurements [31].



Figure 2. 83 Channel Investigational Biomagnetometer

## **EEGLAB**

EEGLAB is a toolbox offering an interactive graphic user interface (gui) which runs under the cross platform MATLAB environment. It is intended for flexible processing of continuous and event-related EEG, MEG, and in general electrophysiological data by employing independent component analysis (ICA) algorithm, time/frequency analysis, and various artifact rejection algorithms and programs such as standard averaging methods [32] [41] .

EEGLAB comes with a detailed tutorial and help notes and a command history function for smooth transition from gui-based data exploration to building batch, running it or custom data analysis. It is freely available under the GNU public license for noncommercial use along with the tutorial, sample data and thorough documentations. Some other features are visualization and modeling event-related brain dynamics, structured programming environment for storing, accessing, measuring, and manipulating any high density and dynamic brain data, and open-source platform for research programmers to share methods with the research community by contributing plug-in functions that show up in the menu [32, 41]. More specifically, available EEGLAB functions are for EEG and MCG data, channel or event information importing, data visualization, pre-processing, independent component analysis (ICA) and time/frequency decompositions. All these functions are categorized in three different layers with the goal of ease of use and efficiency by various types of users. When using top layer functions, the user does not need MATLAB syntax and instead can work with the data using the graphic interface. This is the simplest way to import data, and run it through processing and visualization functions in the main menu under five tabs: File, Edit, Tools, Plot, and Help [32, 41] .

The second layer consists of the EEGLAB command history which is suitable for intermediate users. In addition to using the main menu, these users can use the command history and create

batch scripts when they need to process similar datasets. Menu option functions can also be called through Matlab command lines and depending on how they are called, they run with or without a pop-up window for taking additional inputs or parameters.

The third layer of EEGLAB functions is the opportunity for the user to take advantage of fully documented data processing functions directly for direct computations on datasets with the user's own script. Experienced users can write their own scripts using EEGLAB data structures to call any EEGLAB functions. The best way to take full advantage of EEGLAB is to use all three modes of EEGLAB capabilities described above: GUI-based, history-based, and autonomously scripted data analyses [32] .

### **fMCG and EEGLAB**

fMCG recordings contain much more than needed for FHR and FHRV assessment. They have signals from several sources other than the heart from both mother and fetus. The Independent Component Analysis (ICA) available in EEGLAB is based on an infomax-based ICA algorithm [41] , which incorporates the maximum entropy method by Bell and Sejnowski [42] that maximizes the mutual information between inputs and outputs by only maximizing the entropy of the outputs, and Amari et al learning algorithm which minimizes a statistical dependency among outputs for blind separation of mixed signals [43] . By estimating an optimal linear transformation, ICA maps the multivariate data into temporally independent components with distinct spatial distribution [23] .

In the case of fMCG, ICA is used for filtering purposes, enabling the removal of components that have temporal patterns which associate them clearly with other electrophysiological sources [15] . ICA separates raw biomagnetic signals into maternal cardiac, maternal breathing, fetal

cardiac, fetal breathing, fetal movements and other artifacts according to their spatially distinct electrophysiological sources. It reconstructs specific components in the sensor space to map the location of their corresponding signals [25] and this makes it possible to obtain HRV from the QRS wave and specifically the R-R interval. This algorithm has been independently evaluated and verified for efficiency in artifact rejection of fetal magnetographic recordings and used by several researchers in this field for purposes such as characterizing fetal behavior [23, 44, 45] .

### **KubiosHRV**

Kubios is an advanced software tool for studying the variability of heart beat intervals. It was designed by Kubios OY (limited company) which is a biotech company with the focus of developing software and algorithms for biomedical signal analysis. Several analysis options and user-friendly interface, it is the most popular HRV tool used by many human or animal health, medical, or sports researchers and clinicians in the fields of cardiology, neurology, maternal-fetal medicine, etc. It enables examination of the heart together with the ANS functioning. The most common uses of this software today is in the fields of HRV analysis and neurology as well as sports research in assessing the well-being of athletes [35].

There are currently two versions of this software, Kubios HRV Standard and Kubios HRV Premium. The main advantage of Premium over Standard is that it supports a wider range of ECG and HR data, it offers time-varying options and supports group analyses, and is for scientific and commercial applications. A comprehensive Kubios HRV user manual is available with both versions of the software in which metrics, procedures, settings, etc as well as functional differences between the two versions are explained. With each updated version of the software, the user's guide is updated with a "release note" section which consists of detail descriptions of the most recent updates and changes. This user's guide is accessible on the Kubios website. The website

also has a FAQ/troubleshooting section addressing the most common and recent issues users face with solutions. The main advantage of Premium over Standard is that it supports a wider range of ECG and HR data, it offers time-varying options and supports group analyses, and is for scientific and commercial applications.

System requirements for running Kubios on Windows are the following: a 64-bit operating system with at least 4 GB of RAM and 3-5 GB of disk space, 1024 \* 768 or higher screen resolution, and the MATLAB Runtime R2016b (ver 9.1) because Kubios was developed using this version of MATLAB and was compiled to a standalone application with the Matlab compiler [35]. After registration or purchase is completed at <http://www.kubios.com/>, necessary information for installation and the personal license key are provided. Installation is easy and straight forward and before the first launch, the user needs to activate her personal license key on the same computer [35] .

The user's guide is the best reference to get started with Kubios HRV, however it does not include step by step instructions. This is because there are numerous pathways and applications for using the metrics and analysis options. The user's guide includes an overview of HR and HRV, extraction of heart beat intervals, derivation of HRV time series and other descriptions needed for every researcher to better interpret the data and use the available analysis options. It also includes descriptions of types of input data that are supported and approaches for saving and analysis of outputs and results, software features and operational interface. Instructions for setting requirements for different analysis options and other details needed to learn all the functionalities of the software are also included.

The user's manual also contains two sample runs and pre-processing and analysis methods in the time-domain, frequency-domain, nonlinear and time-varying categories for more thorough and practical aspects of working with and making the most of raw data.

### **Data Collection**

Each recording session is conducted individually. Before starting the pregnant participant is asked to remove pieces of clothing that contain metal or jewelry which could interfere with the recordings. Then she is seated in a reclined posture facing the biomagnetometer and both the seat and the biomagnetometer are adjusted so that the maternal abdomen fits inside the concave surface of the sensor array with minimal contact, ensuring the participant can easily take deep breaths without feeling any discomfort or pressure, particularly on the vena cava. Legs are supported via adjustable foot pedals, hands are rested against arm cushions, and optional head rest and back support is available. Each recording lasts for 30 minutes, throughout which the participant is monitored or if necessary interacted with, via camera and microphones in the shielded room.

The biomagnetometer has 83 channels. This number of channels is necessary because the recorded signal is a combination of signals from numerous sources such as maternal or fetal heart, fetal brain or eyes, breathing or extremities movements and other in utero activities. Without these many sensor channels it would not be possible to record and then separate all the signals because of insufficient information captured by the recording.

Data is acquired with a 1200 Hz sampling rate and a recording filter of 0-75 Hz. Afterwards, digital filtering is performed offline with bidirectional fourth-order Butterworth filters between 0.5 and 40 Hz. The resulted raw data is a combination of several maternal and fetal signals with different sources such as maternal breathing, uterus smooth muscle contractions. By visual



inspection, maternal and fetal MCG are distinguishable, even though the peaks overlap at times and could prevent the correct identification of all R-peaks [31] .

After opening EEGLAB and running it in MATLAB, by selecting “load existing dataset” under the tab file, the fMCG recording in .set format is loaded. Then under the tab “plot”, “component activities” are plotted. The channels record mixed signals from several sources such as maternal and fetal cardiac signals, diaphragm movements, nonnutritive suck, and maternal muscle contractions, and etc. When EEGLAB is plotting component activities, in fact it is performing ICA to decompose the mixture of signals recorded by the sensors into temporally distinct (maximally independent over time) components each of which normally display one specific signal [31, 41] .

After waiting a few seconds for ICA process to be completed, the plot of all components are loaded and the independent components are visually inspected in order to recognize all the components of interest. Figure 3 shows a typical component activities plot. Using previous work of several researchers in characterization of fetal behavior using fetal magnetocardiography, several components such as fetal cardiac, maternal cardiac, fetal hiccups, maternal uterine muscle contraction, fetal nonnutritive suck, fetal dMMG and eye movement can be recognized [22-25] . In Figure 3, 10 seconds of fMCG data with activities of the first 11 independent components are shown. Maternal cardiac components are seen in IC1 and IC2, fetal cardiac components are seen in IC3, IC4 and IC5.

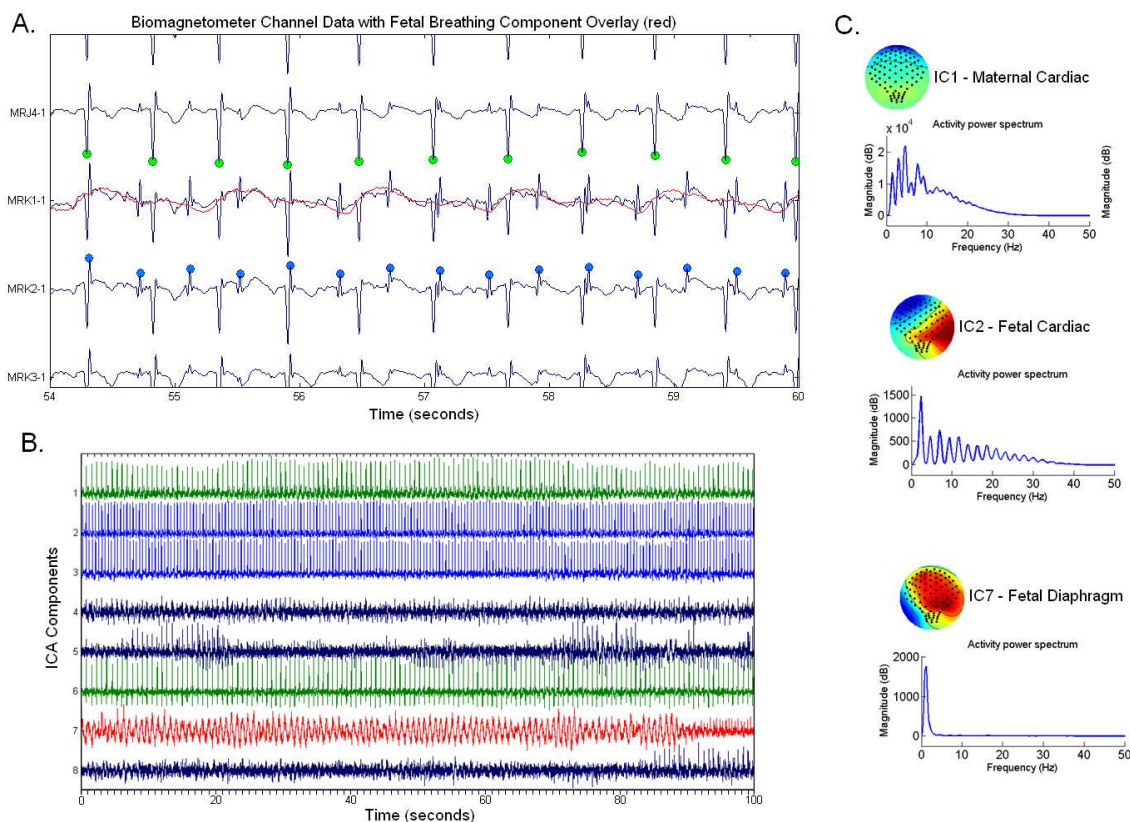


Figure 3. Component activities, EEGLAB

After visually inspecting and identifying the fetal cardiac components, they need to be extracted and isolated from the rest of the components. A good component is one that is consistently showing fetal cardiac recordings preferably for the entire recording time. If there are more than one such components, all must be retained in order to maintain as much information as possible. Under the tab “tool” in the main menu, picking the option “remove components” opens a window in which the components to retain or the ones to remove can be specified. The output of this step is another .set file which is saved as a different name and automatically loaded in EEGLAB. In order to use this data for obtaining IBT time series, HR and HRV, a .text file is needed. Therefore this file is exported to a text file containing the RR data.

Many times especially in early weeks such as 28 weeks and prior, due to the small size of the fetus and occurrence of numerous and quick movements, the signal is not retained in any one components for the entire recording. Therefore, there are no good components to isolate and export. For example, depending on how the fetus moves, fetal cardiac signal may be visible in IC2 for the first 6 minutes of the recording and then be transferred to IC4 for the next 4 minutes. This might happen several times during a 30 minute recording.

In this case to maintain the entire signal as much as possible and yet prevent contamination of components into each other, the chosen components could be extracted and reconstructed together. But an additional step is required in which after extraction of the best components, the channel data is plotted to identify and extract appropriate channels which contain the desired signal. Using this step, the signals are reconstructed from the channels and instead of exporting components to text file, channel data are exported to text file. A good channel is a channel in which RR peaks are recorded consistently for the entire recording. It is preferred that these RR peaks are positively recorded in this channel, and if that is not the case, a channel must be picked that has either positive or negative RRs consistently for the entire recording. A channel in which RR peaks are flipped up and down multiple times is not useful for further processing. Extraction of good channel(s) helps remove any other signals from undesired sources or noise which lead to unfavorable ICA outputs in the first place.

### **Edit Preferences**

The settings and specifications for how to process and analyze ECG and RR interval data can be edited and set permanently in “Preferences”. Preferences has 4 different groups. The first one is User Information in which the name, last name, affiliation, and etc. of the person who performs the analysis, are specified to be shown in the report sheet as well as ACCII text file [35] .

The second group is Input data & Pre-processing which allows the input data type to be set to any of the formats compatible with Kubios. Signal type can be specified to either ECG or PPG which determines the heartbeat detection procedure. With ECG signals, QRS detection options let the user set the polarity of R-wave. This comes in handy especially when the exported fMCG channel has inverted signals where the R peaks are flipped down and therefore the RR intervals in the text file are negative. The prior guess for RR interval could also be designated as automatic, letting Kubios detect the R-waves polarity. Most of the time if any issues come up in identifying the R-waves, the automated polarity can be changed for better results. This might be the case when processing data other than adult humans (such as fetal data or small animals) where mean RR interval is shorter [35]. The interpolation rate and detrending method is also set here.

### **Analysis Options**

The analysis options settings are the most detailed and significant section of preferences which influence the results of processing. In this section first the general analysis settings such as RR Interval Samples specifications and the mode of updating results are selected. Then the analysis which is intended for the data is selected and its details are specified. For time-domain, frequency-domain and nonlinear analysis, the option standard analysis is appropriate. Time varying analysis could be picked separately. Selecting the method here prevents a waste of time for processing that is not required. To manipulate samples, their numbers, their processing manner, RR interval samples details are used.

Once the analysis method is selected, further details and specifications are filled out. In time-/frequency-domain section, the number of beats for taking the Max/Min HR (window width of the moving average filter) and NNxx and pNNxx threshold are stated. The ranges for frequency bands can be set depending on what type of HR data is being analyzed (humans, animals, etc). the

points/Hz in frequency domain correlate with the width of the moving average filter by default unless interpolation is intended, which should be controlled with changing the points in frequency domain. FFT spectrum method is also selected here. Generally for HRV spectral analysis, the use of Lomb-Scargle periodogram is recommended. In the nonlinear analysis section, it can be specified whether or not the processing is to be performed on detrended RR interval data. With unchecking of the first box in this section, even though RR interval data is detrended, but the nonlinear metrics are calculated from non-detrended data. The settings for calculating ApEn and SampEn, short term and long term variability in DFA and recurrence plot and correlation dimension details are set up here. In the time varying section, the user can limit the time-varying analysis to be performed only for select samples to increase speed. For the window of time-varying analysis, the width and grid interval (the time by which the window moves with each step) can be set in seconds. For example, if the whole interval is 40 minutes and the analysis is to be performed on 5 minute sections of this interval, both the width and grid interval should be 300 seconds. Spectrum estimation method can be changed from default which is the spectrogram to Kalman smoother method if desired.

### **Report Settings**

The report settings are available to choose which of the analysis results are to show up in the report. Details such as the report paper size, color theme, and format of numbers for SBSS friendly reports can also be changed here. All settings and modifications specified in preferences are saved with the OK button. Once the preferences are saved, they will apply to the next session until the program is restarted or Close File is selected. Most of the options in preferences can also be changed in local settings for each analysis method for a current session, but doing this in preferences is more efficient and permanent. The preference directory paths of searching the data

file or saving the results and saved preference options are preserved in user specific folders. For windows 7, 8, or 10 these paths are the following:

HRV Standard: C:\Users\\AppData\Roaming\Kubios\KubiosHRVStandard

HRV Premium: C:\Users\\AppData\Roaming\Kubios\KubiosHRVPremium

### **Specific Preference Settings for This Thesis**

After entering the user information, in the input data & pre-processing preferences are set according to the following table (everything not specified here as well as the entire report settings remain as default),

Table 1. Input Data and Pre-processing Settings

Data type	EKG ASCII files
R-wave polarity	automatic
Prior guess for RR interval	automatic
Interpolation rate	10 Hz
Detrending method	None

For the analysis options, both the General analysis and Time-varying analysis are selected. Further details are shown in the following table,

Table 2. Analysis Options Settings

Number of samples	1
Default sample length	300 s
Sample analysis type	Single samples
Update mode	Automatic

Table 3. Time/Frequency Domain Settings

Min/max HR as average of	5 beats
Threshold for NNxx and pNNxx	10 ms
VLF	0 – 0.08 Hz
LF	0.08 – 0.4 Hz
HF	0.4 – 1.5 Hz
Points in frequency- domain	300 points/Hz
Window width	300 s
Window overlap	50 %
AR model order	16
Use spectral factorization	No

Table 4. Nonlinear Settings

Embedding dimension (for ApEn and SampEn)	2 beats
Tolerance	$0.2 \times SD$
Short term fluctuations (N1)	4 – 12 beats
Long term fluctuations (N2)	13-64 beats
Embedding dimension (for recurrence plot and correlation dimension)	10 beats
Threshold	$3.1623 \times SD$

Table 5. Time – Varying Settings

Window width	60 s
Grid interval	1 s

After saving preferences the first step of opening the RR interval text files obtained from EEGLAB is to select “RR Interval ASCII files (\*.txt, \*.dat, \*.csv) out of the 6 general data formats supported by Kubios.

Text file obtained from EEGLAB processing is the starting point of the data analysis using Kubios. Kubios supports several data formats including RR interval text files \*.txt and Kubios HRV Matlab MAT files \*.mat files which are of interest in this project [35] . For kubios to process



RR interval text files, RR intervals must be measured/stored in beat-to-beat. This is why all the filtering and processing in EEGLAB are necessary. HRV analysis cannot be performed on average HRV data. Kubios works with more than one type of input in the RR interval text files. Here the text files obtained from EEGLAB contain one column showing the RR interval values in order. These values are given in milliseconds.

The Kubios version used for this analysis is Kubios HRV premium version. The user interface window of Kubios HRV has three sections: The RR interval series options, the data browser segment, and the results view segment [35]. The RR interval series options can be used to take advantage of artifact correction, modifying and tailoring of samples for analysis, and removing trend components .

### **Artifact Correction**

For artifact correction there are two options, 1) Automatic Correction and 2) Threshold Correction. The automatic correction is an algorithm which identifies artifacts such as missed or misplaced beats or ectopic beats (premature ventricular beats) in an RR interval series. The threshold correction however only examines each beat interval against a local mean RR and considers it an artifact if it is above the given threshold. This threshold should be designated specifically for each individual because variability of RR intervals is different between different people.

The artifact correction method used here is automatic correction. Once automatic correction is selected, the summary of corrections to be made on the RR interval are shown in green in the data browser segment as the number of beats and their percentage. Artifact correction essentially produces artificial values to replace the artifacts and therefore incorporate interpolated values into

the RR interval data. Caution must be taken that the percentage of corrected beats should be below 5%. Otherwise results and their interpretation will be notably distorted. If this number is 5 % or more, the RR interval series must have been too corrupted for further processing. By clicking the apply button these corrections are implemented, without affecting the normal RR intervals. The corrections are made based on a piecewise cubic spline interpolation method.

By comparing the time-domain results with and without artifact correction the necessity and significance of artifact correction can be verified. The effect of artifacts on parameters such as SDNN, RMSSD, and TINN cannot be ignored and therefore care must be taken to correct them before the analysis [35] .

### **Samples for Analysis**

In the Samples for Analysis Section, samples can be added or removed, and multiple samples can be generated out of a single recording for performing simultaneous but individual analysis and obtaining results in a single Kubios HRV report. The start time and length of each of them can be set as desired. If it is needed, several samples can be merged into and analyzed as one long sample. This feature is useful for studies involving comparing different behavioral states which are displayed by the fetus throughout one recording session.

### **Remove Trend Components**

This feature offers methods for removing any low frequency baseline trend components that is in the RR interval time series. Options include a method called smoothness priors or removal of the first, second, or third order linear trend. The smoothness priors method is a time-varying high pass filter and therefore the smoothness of the removed trend can be manipulated by adjusting the Lambda parameter which determines the cut-off frequency. The cut-off frequency is shown with

the Lambda value edit box and a bigger value of Lambda leads to a smoother removed trend. Before removal of the trend, it is shown as a red line on the analyzed RR data sample [35].

### **The Data Browser Segment**

The data browser segment shows the measured ECG signal and the derived RR Series. Both series are shown for the whole time of the dataset. The range of axes can be changed by writing values in the boxes next to them. By using the lock button on the bottom right corner, both series can be scrolled together. The grey patch in the RR chart shows the ECG range and it can be moved along the X axis. Other than displaying of ECG and RR data, the data browser segment's purpose is to allow artifact correction. If the ECG is available in addition to the RR data, artifact correction can also be performed manually. Each + mark on the ECG signifies an R-wave and therefore using the mouse and precise clicking, each + can be moved if it is out of place and additional R-peak markers can be designated where they are missing. The placement of the markers does not have to be completely manual, once they are clicked on, they will be designated to the nearest ECG maximum with a click. These changes simultaneously show in the RR interval series [35]. The data browser segment also has options for printing the ECG for a specific range recording or changing the RR data type to HR.

### **The Results View Segment**

This segment shows the results of analysis for the analyzed RR interval sample. Time-domain, frequency-domain, nonlinear and time-varying results and graphs are available with the push of a button for each. With every change in the settings or sample(s) of the RR interval data, the results are automatically updated. This automatic update takes a few seconds depending on the size of the samples. The smaller the length and the number of the samples, the higher the speed of processing.

If this is not necessary and a higher speed is in priority instead, unchecking the “auto-refresh results” option can stop the updating. The results can still be updated by clicking “refresh” when preferred [35].

### **Time Domain**

The time domain results view shows one table and two histograms. The table includes calculated variables such as Mean RR, STD RR (SDNN), Mean HR, STD HR, Min HR, Max HR, RMSSD and etc. If detrending has been applied during the processing, all parameters except Mean RR and Mean HR will be computed for the detrended RR series.

The histograms have boxes below them that allow the user to set RR (s) and HR (bpm) fixed axes limits. These settings can be entered in “Preferences” in Kubios once without the need to be entered every time Kubios is opened. If they are not specified, then the minimum and maximum values in the data are used to auto-scale the histograms [35].

### **Frequency Domain**

Frequency domain results view displays one table and the spectra of the FFT (Welch’s periodogram) and AR spectrum estimation methods (performed on detrended RR series) with their numbers shown in the table on their left. In Premium version only, Lomb-Scargle periodogram can be chosen instead of FFT based on Welch’s periodogram. The frequency axes are 0-0.5 Hz by default and otherwise the range is 0 - upper limit of HF band+0.1 Hz.

When ECG is measured, in addition to the results in the table, electrocardiogram derived respiration (EDR) which is an approximation of the respiration frequency is also calculated and shown separately below the spectrum options. It is indicated with a vertical line in the spectra as well. EDR can be hidden using the checkbox below the spectrum options boxes.

The adjustable settings for frequency-domain results view can be used to establish limits of the power axes. Also the limits of very low frequency (VLF), low frequency (LF), and high frequency (HF) bands can be changes and any adjustments in this window are kept only for the current session. All changes made here will carry on to the report sheet for the current session. To maintain settings and changes permanently, they must be implemented by using “Edit Preferences”. The default values for the bands are VLF: 0–0.04 Hz, LF: 0.04–0.15 Hz, and HF: 0.15–0.4 Hz according to the guidelines by “Task Force of The European Society of Cardiology and The North American Society of Pacing and Electrophysiology” [35].

### **Nonlinear**

The nonlinear results view consists of a table of all the calculated nonlinear variables. The successive RR intervals variability is demonstrated visually by the Poincare plot. The Detrended fluctuations (DFA) plot presents the detrended fluctuations and their slopes against  $n$  on a double logarithmic graph.

### **Time-varying results**

Time varying results show the time varying trend of any selected time domain, frequency domain, or nonlinear variables. Color map of the time-varying spectrum is displayed along with a color bar for reading different colors for different power values. The window width and grid interval can be adjusted. The time varying spectrum can be calculated with one of the two methods of spectrogram and Kalman smoother. Under the box for choosing the spectrum method, adaptation coefficient which changes the adaptation speed of the algorithm [35].

## Our processing

The samples for analysis are 30 minutes long. For both maternal and fetal data, all 4 analysis methods are performed on the entire 30 minutes and the Kubios 3 types of reports are obtained. The ASCII text file, the PDF report, the .mat file. Then the SampEn, ApEn and MSE are extracted for analysis. Examples of parts of the PDF report are demonstrated in figures 4 and 5.

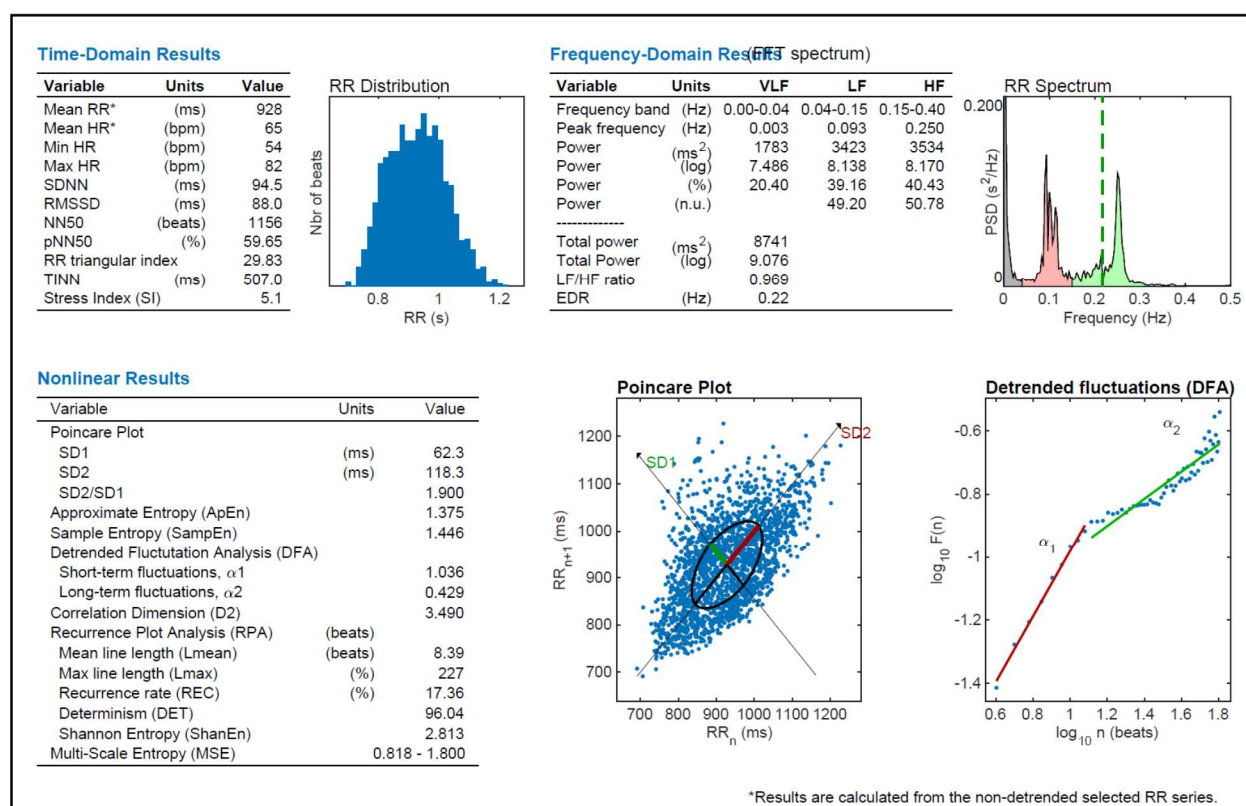


Figure 4. Time-domain, frequency-domain, and nonlinear analysis results in Kubios report

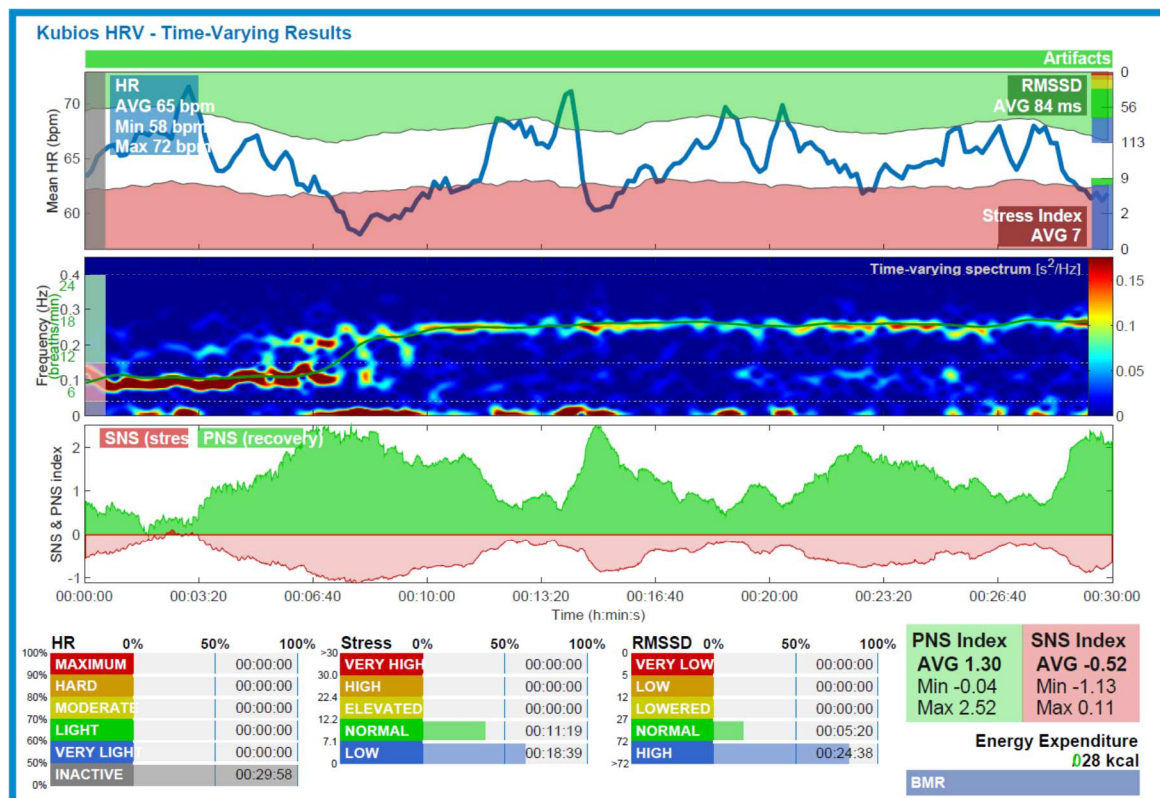


Figure 5. Time-Varying results in Kubios report

## HRV Metrics and Methodologies

There are several metrics and methods for analyzing fetal heart rate variability such as time domain, frequency domain, nonlinear, and time-varying methods [35] [31]. All these methods use the RR interval series for calculations. **Time domain methods** is the most preliminary analysis applied to HR and signify general changes in fetal HRV and average HR. The metrics of this approach are mean HR, SDNN, SDD (SD of HR), RMSSD, NN50 and pNN50. **Frequency domain analysis** calculates a power spectrum density (PSD) to compute the absolute and relative VLF, LF, and HF band powers, normalized LF and HF band powers, the LF/HF power ratio, and peak frequencies for each band. **Nonlinear methods** are some of the most recent and in depth

HRV analysis methods which are based on measures of ApEn and SampEn, DFA, Poincare plot, Multiscale entropy (MSE). **Time- varying methods** focus on trends of time domain, frequency domain, and nonlinear metrics [31, 35]. The last and most recently developed approach is **Stress index and PNS/SNS indexes**

### Time domain

Mean RR interval is what is referred to as mean heart rate (HR) in most literature. It is the mean of Time interval between successive electrocardiogram R-waves (RR interval, same as IBI). An example of HR time series and RR series from Kubios are shown in figure 6. The rest of the time-domain variables are for estimating the variability within the RR series. SDNN is the standard deviation of RR intervals, representing both short-term and long-term, therefore overall variability, which is calculated according to Equation 1 [35],

$$SDNN = \sqrt{\frac{1}{N-1} \sum_{j=1}^1 (RR_j - \overline{RR})^2}$$

Equation 1

In which  $RR_j$  is the  $j$ th RR interval and the overall number of successive intervals is denoted by  $N$ . Another standard deviation is SDD, standard deviation of successive RR intervals which signifies short term variability and is computed using Equation 2,

$$SDD = \sqrt{E\{\Delta RR_j^2\} - E\{\Delta RR_j\}^2}$$

Equation 2



which is equal to the root mean square of successive RR interval differences (RMSSD) for a stationary RR series,

$$RMSSD = \sqrt{\frac{1}{N-1} \sum_{j=1}^{N-1} (RR_{j+1} - RR_j)^2}$$

Equation 3

RMSSD calculates beat to beat variation and therefore signifies short term variability [16].

NN50 is another time-domain metric which indicates the number of successive intervals which vary by more than 50 ms and is sometimes represented as its relative value, pNN50,

$$pNN50 = \frac{NN50}{N-1} \times 100\%$$

Equation 4

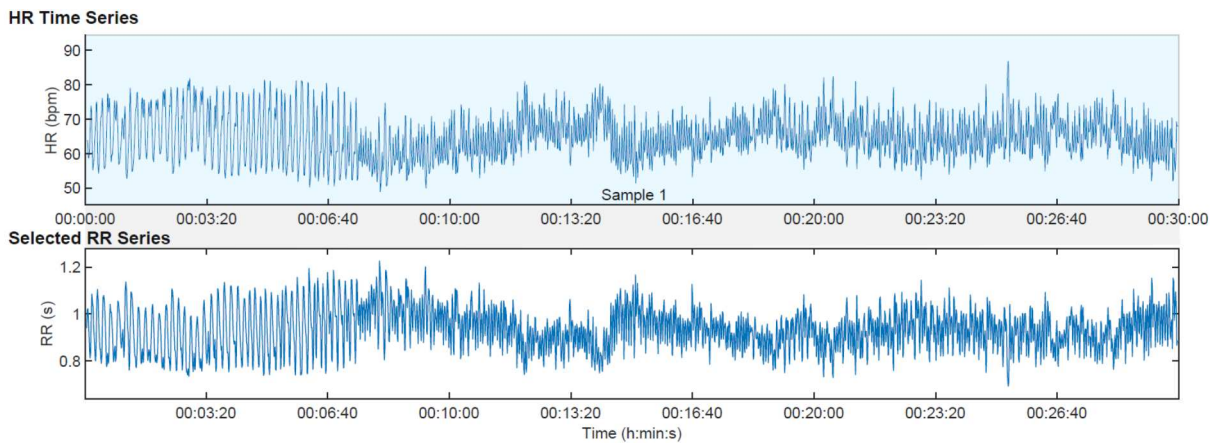


Figure 6. HR time series and RR series example

## Frequency Domain

As for the frequency domain parameters, Very Low Frequency (VLF) with the default value of 0 - 0.04 Hz, low frequency (LF) as 0.04 - 0.15 Hz and High Frequency (HF) as 0.15 – 0.4 Hz are used for adult HRV. For fetal HRV these frequency bands are respectively 0 – 0.08 Hz, 0.08 – 0.4 Hz, and 0.4 – 1.5 Hz [35]. Frequency domain metrics are obtained from a spectrum estimate for each frequency band. An example spectrum is shown in figure 7. These metrics are: absolute and relative powers of VLF, LF and HF bands; LF and HF band powers in normalized units; the LF/HF power ratio; and peak frequencies for each band [46]. In addition LF/HF ratio and EDR are calculated. Frequency domain analysis of HRV dissects sympathetic and parasympathetic activity by some means, but it is very sensitive to missing data points [47].

The HF band is attributed to vagal control because the efferent vagal activity is the biggest contributor to the HF component of HRV [46, 48]. HF component is mediated by parasympathetic control and is therefore

centered at respiratory frequency and has the range of 0.15 – 0.4 Hz. It is referred to as respiratory band because it corresponds to the respiratory HRV. HF power is closely correlated with pNN50 and RMSSD. With the inhibiting of the vagus nerve stimulation by the cardiovascular center during inhalation, HR increases and during exhalation is decreases. Total parasympathetic blockade eliminates the HF oscillations [49].

The LF component reflects both vagal and sympathetic heart rate regulation and baroreflex activity. There is not agreement on whether the PNS activity is has the dominant influence on this component or the SNS [46, 48, 49]. The absolute LF power should not be relied on as a direct

indicator of sympathetic activity but both normalized LF and HF powers (n. u.) respectively show valid links to sympathetic and parasympathetic activities [46, 48].

The integration of various autonomic and humoral control loops such as the thermoregulatory processes and renin-angiotensin system is signified by VLF component [46, 48]. There is not yet definite consensus on the physiological sources of the activity in the VLF band. The heart's intrinsic nervous system and SNS influence affect the VLF rhythm. PNS control certainly influences VLF power because in the case of Parasympathetic blockade, VLF component almost entirely disappears. Sympathetic blockade has no influence on VLF power [49]. The complex relationship between SNS and PNS nerve activity means that the ratio between LF and HF power will not always index autonomic balance [49].

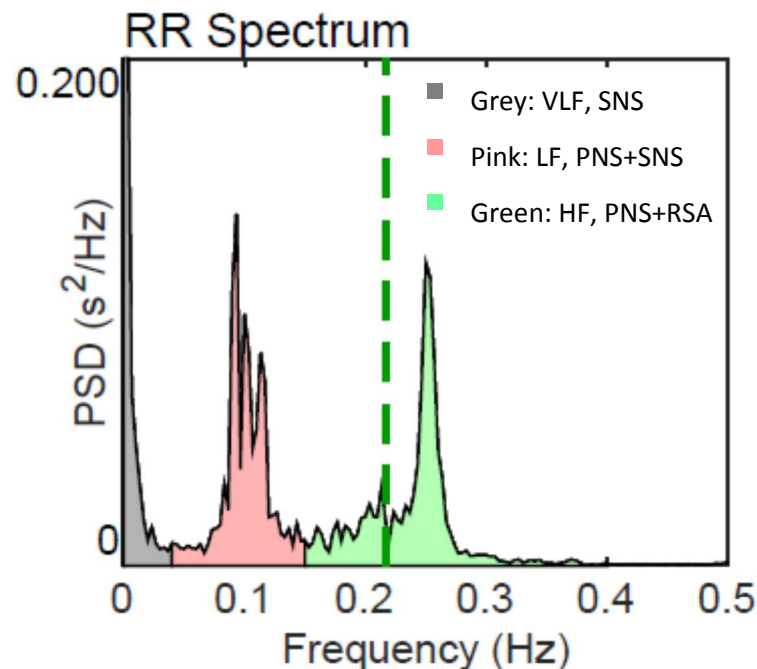


Figure 7. Frequency domain spectrum example

## **Nonlinear Methods**

Sample entropy (SampEn), approximate entropy (ApEn), and Multiscale entropy (MSE) are nonlinear indices and approaches for assessing the level or irregularity in HRV data. Poincare plot (or a recurrence map) is also another nonlinear approach of demonstrating short term and long term variability [31] [50].

### **ApEn**

According to the definition of Kolmogorov-Sinai (KS) entropy [50] in system dynamics, entropy is the rate of information production. The Approximate Entropy (ApEn) is an entropy based complexity measure that is applicable to clinical cardiovascular datasets or several similar types [31]. Developed by Pincus for analysis of short noisy time series [50] from theory developed in the area of nonlinear dynamic analysis and chaos [47] and originated from efforts of Grassberger and Procaccia [51] and Eckmann and Ruelle [31, 50], ApEn evaluates the time series for similar epochs. This nonlinear analysis is approximately the negative natural log of the conditional probability that a dataset of length  $N$  which has already repeated itself within tolerance  $r$  for  $m$  points, is going to again repeat itself for  $m+1$  points [47]. In other words it has an inverse relationship with the conditional probability that two sequences that are similar for  $m$  points will maintain this similarity (within the tolerance  $r$ ) at the following point [31].

Approximate Entropy (ApEn), is a nonlinear method for assessing the irregularity of a signal. Therefore, the larger its value, the more irregular the signal is. The value of ApEn depends on  $m$ ; the length of the vectors,  $r$ ; the tolerance value, and  $N$ ; the length of the dataset. It is calculated according to Equation 5,

$$u_j = (RR_j, RR_{j+1}, \dots, RR_{j+m-1}), \quad j = 1, 2, \dots, N - m + 1$$

Equation 5

$m$  is called embedding dimension and in Kubious, is set to 2 by default.  $N$  is number of measured RR intervals which is the length of the dataset and the larger it is the closer the ApEn gets to its asymptotic value.  $U_j$  are a set of vectors with length  $m$  the distance between which is computed as,

$$d(u_j, u_k) = \max \left\{ |RR_{j+n} - RR_{k+n}| \mid n = 0, \dots, m - 1 \right\}$$

Equation 6

Next,  $C_j^m(r)$  is calculated as the relative number of vectors  $U_k$  for which this distance is less than or equal to  $r$  which is the tolerance value. The tolerance value should be set as a fraction of SDNN, the standard deviation of the data, and this makes ApEn a Scale-invariant measure [47]. This generates sufficient consistency for the comparison of different types of data. Generally, it is set at  $r = 0.2SDNN$  and thus this is its default value in Kubious,

$$C_j^m(r) = \frac{\text{nbr of } \{u_k \mid d(u_j, u_k) \leq r\}}{N - m + 1} \quad \forall k$$

Equation 7

The value of  $C_j^m(r)$  is between or equal to  $1/(N - m + 1)$  and 1. Taking the natural logarithm of  $C_j^m(r)$  and averaging over  $j$ , we get:

$$\Phi^m(r) = \frac{1}{N - m + 1} \sum_{j=1}^{N-m+1} \ln C_j^m(r)$$

Equation 8

Approximate entropy is the difference of subsequent values of  $\Phi^m(r)$ ,

$$ApEn(m, r, N) = \Phi^m(r) - \Phi^{m+1}(r)$$

Equation 9

This algorithm [35] considers each sequence as a match to itself . This match is counted and therefore erroneously implies more similarity and therefore less complexity than is actually present. This is precisely why ApEn is considered to have bias and thus first, depend on the length of the dataset and second, to suffer from lack of relative consistency. The first is problematic because it leads to lower values of ApEn than estimated for shorter datasets. The second means even though the algorithm of ApEn, and specifically the designation of r is intended for consistency and validity of comparison between datasets, this is practically not the case. The relative relationship of the value of ApEn in two datasets will not remain the same for all conditions tested [31].

### **SampEn**

Sample Entropy is a measure of time series regularity similar to ApEn but it carries several improvements. To interpret their role indirectly, one could say both the ApEn and SampEn in fact look for how much the data did not come from random processes. There are several words for this interpretation such as complexity, regularity, or order [35] .

This entropy measure is applicable to a time series datasets sampled from a continuous process [31] . For eliminating the issue of self-matching which in essence means comparing data with themselves [31],  $C_j^m(r)$  is computed as follows,

$$C_j^m(r) = \frac{\text{nbr of } \{u_k \mid d(u_j, u_k) \leq r\}}{N - m} \quad \forall k \neq j$$

Equation 10

In the next step, averaging gives,

$$C^m(r) = \frac{1}{N - m + 1} \sum_{j=1}^{N-m+1} C_j^m(r)$$

Equation 11

and then SampEn is calculated according to,

$$\text{SampEn}(m, r, N) = \ln(C^m(r)/C^{m+1}(r))$$

Equation 12

In Kubios, the default values for r and m are the same as they are set for ApEn. SampEn was developed with the purpose of reducing the bias of ApEn. Additionally, for random numbers with known probabilistic content across a broad range of operating conditions, SampEn is in closer agreement with the theory (than ApEn) [35]. As stated, this method does not count self-matches while calculating the conditional probability which was discussed above. In a sense, a lower SampEn than ApEn shows there has been more self-similarities in the dataset, and disregarding those has led to this lower value [31] .

SampEn also is computationally simpler than ApEn and its algorithm requires one-half of the time required for ApEn. SampEn computation contains no template-wise approach to calculate conditional probabilities. It only requires that one template finds a match with length of  $m+1$ . It is very independent of the length of the recording and therefore it shows relative consistency in cases where ApEn does not [31]. In other words, if with a set of designated values for  $m$  and  $r$ , dataset A has lower SampEn than dataset B, this will remain the case with a different set of  $m$  and  $r$  values [47]. More specifically ApEn lacks relative consistency because data sets with less regularity have fewer matching templates and are more impacted by the bias due to self-matches. SampEn analysis of the same data, on the other hand, reports correctly over the whole range of  $r$ . Practically SampEn is a statistic that counts events. Each time there is similarity between two vectors, this is considered an event. The only instance in which relative consistency would be absent in this analysis is when these events are sparse. Also for very short recordings residual bias occurs due to nonindependence of templates. However there have not been any cases in which ApEn has relative consistency but SampEn does not. Due to these improvements, SampEn has enhanced accuracy over ApEn and this makes it more useful in analysis of experimental clinical cardiovascular and other biological time series [31, 35].

ApEn and SampEn both can be calculated analytically for series of random numbers and in such circumstances their values are nearly identical. In fact if these random numbers are distributed uniformly, ApEn and SampEn should give identical results, and with any other distributions they turn out somewhat different from each other [31].

One advantage of SampEn analysis is that it is not prone to missing data points. This is significant and useful especially regarding neonatal HRV and the fact that usually loss of even small data sections interferes with complexity and regularity measures in truly deterministic data.



There are some additional considerations, precautions, and shortcomings about both ApEn and SampEn. First, there are no guidelines for choosing the optimal values of  $m$  and  $r$  for guaranteeing an acceptable Confidence Interval around the SampEn estimate. Even though they can be optimized this area is largely unexplored and this is one of the issues associated with SampEn [47].

One systematic approach developed by J. S. Richman and J. R. Moorman [31] gives a new metric of entropy estimate's efficiency. This process first finds a range for  $m$  by either fitting AR models or through reflecting on the underlying physical processes. Next, SampEn is computed for several values from a range of  $r$  and the one that maximizes the efficiency criteria is chosen. This method is only an example and not valid for all datasets for which SampEn analysis is applicable [47].

Second, differences in entropies should not always be accepted as a result of differences in regularity and complexity. With reduced variability entropy falls and this could be due to either an increase in regularity (decrease in complexity) or outliers that affect the SD and therefore the variance.

This could cause a clinical issue because it is observed that HR and surrogate data fall when spikes occur. It is proved by [47] that specifically neonatal HR data is affected by spikes as much as by increased regularity and may be even more. This explains why reduced variability and transient decelerations in fetal and neonatal HR records bring upon lower ApEn and SampEn. This sometimes causes confusion especially when regularity is not otherwise indicated or visually observed. Thus it is always important to keep in mind the reasons for this reduction that are irrelevant from regularity decrease in complexity. Both ApEn and SampEn, are therefore vulnerable to outliers, even though initially ApEn was claimed to be robust against them. This

gives perspective as to why caution must be taken when drawing conclusions from traditional nonlinear dynamics of HR data.

Reduced variability and transient decelerations could signify ANS dysfunction or defective and incomplete intracellular signal transduction processes, but its mechanism is not known. Even though SampEn does not help with identifying the mechanism, it can still be used as a general measure for health of infants and newborns through monitoring of high risk fetuses and newborns for cases such as Sepsis and evaluating the burden of illness [47].

Even though sample entropy (SampEn) is less dependent on the length of dataset, both ApEn and SampEn give a higher value of entropy for pathologic datasets that show less complexity than healthy time series. This is because these metrics are both on a single scale which is the shortest one, and based on the function's one step difference. Therefore, using the past history of time series, they indicate the uncertainty of the next new point [50]. Both metrics fail to account for features of structures on scales other than the shortest one.

### **Multiscale Entropy**

So far several metrics and methods for heart rate and heart rate variability were discussed. In the developing of each of these metrics, scientists and engineers have tried to overcome several challenges and eliminate shortcomings of each previous method. Quantification of complexity of biological systems using physiologic time series has been always a significant focus of researchers. However previous heart rate metrics do not offer any insights into this problem. The reason is that the multiple time scales of healthy physiologic dynamics is overlooked by these methods. They quantify the orderliness of a time series and imply that the more disorder and randomness, the higher the value of entropy is. Thus they assume highest value of entropy for a randomly generated

set of numbers, attributing the highest entropy to the least complex and correlated system. In other words, these cannot distinguish between randomness in pathologic conditions and antagonistic but sophisticated and correlated dynamics of healthy systems. Mostly the previous metrics have been employed in assessing complexity even though they count any lack of similarity and regularity as complexity when in a living system this is not always the case. The reason for the importance of measurement of complexity is that it signifies pathologic dynamics such as aging which degrades physiologic information content and deteriorates the adaptive ability of organ systems. Dynamic physical and biological systems rarely display features of perfect regularity and complete randomness. Multiscale entropy retains the information overlooked by conventional measures because it captures dynamic characteristics displayed by these systems on multiple spatial and temporal scales [50]. In attempts to solve this problem, Costa et al [50] created another methodology with the intent of recognizing pathologies and the difference between random uncorrelated noise with long-range correlated noise [35, 50].

Multiscale Entropy (MSE) is an extension of SampEn while taking into account the multiple time scales in living systems. This method is based on Zhang's proposed approach using Shannon's entropy which did in fact show differences between correlated and uncorrelated noise, but was not suitable for physiologic signals since it is only applicable to relatively long and nearly noise-free datasets and does not work for finite length noisy data such as cardiac recordings [35, 50].

MSE calculation involves two major steps, first is a coarse graining process and second is computation of SampEn for each coarse-grained time series. Starting with a one-dimensional discrete time series, consecutive coarse-grained time series are created, averaging the data points within non-overlapping windows of increasing length according to the following equation:

$$y_j^{(\tau)} = \frac{1}{\tau} \sum_{i=(j-1)\tau+1}^{j\tau} x_i \quad 1 \leq j \leq \frac{N}{\tau}$$

Equation 13

In which  $\tau$  is the scale factor. The length of resulted coarse-grained time series is their original beat-to-beat RR interval time series length reduced by a factor of  $\tau$ . Afterwards the SampEn is computed for each of these time series and the value is returned as a function of  $\tau$ . Clearly, the scale 1 MSE is the same as SampEn. The concept of course graining is shown in figure 8. Larger scales are obtained by accumulating neighboring NN intervals leading to lower time resolutions (low-pass filter) and increasing investigation time horizons according to the coarse graining procedure [48]. Using MSE, the complex structures across multiple time scales in correlated noise are recognized and therefore distinguished from the randomness in white noise [48].

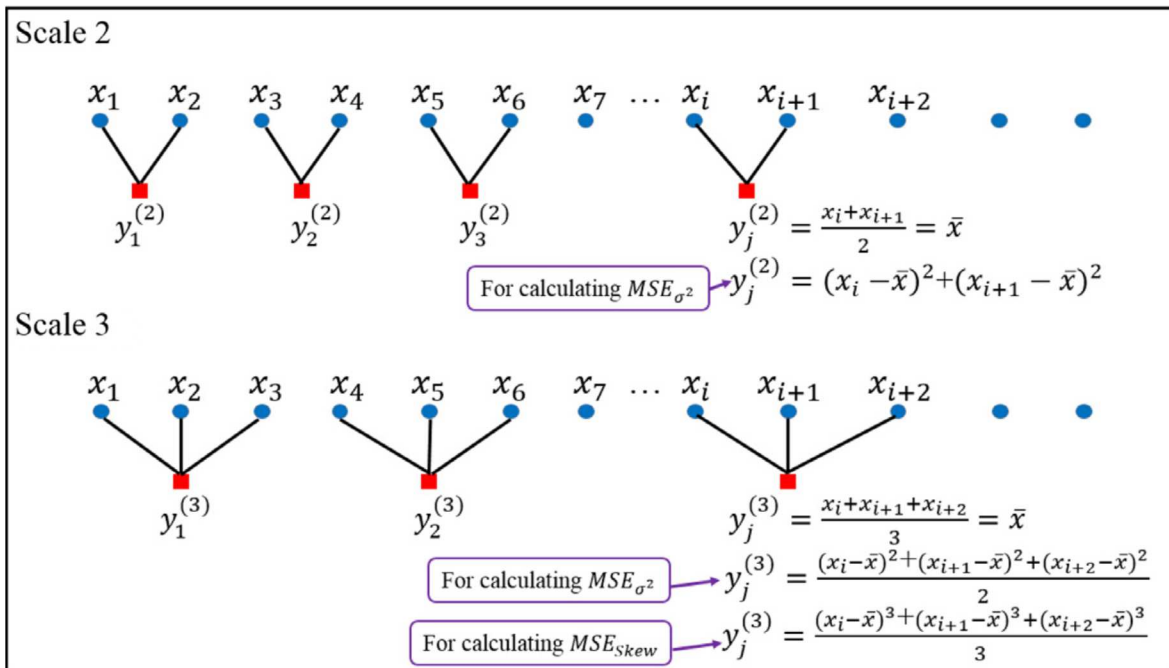


Figure 8. Course-Graining Procedure [52]

MSE distinguishes between healthy and pathologic systems and between correlated and uncorrelated white noise and each of their complexity levels. Pathologic systems have a reduced complexity which could be signified by either increased orderliness and decreased variability or increased randomness and therefore increased variability due to cease of correlated and adaptive coupling of organs and organ systems. It is therefore not surprising that multiscale entropy also decreases with old age [53]. Physiologic complexity is a concept more sophisticated than just lack of order or regularity and that is why measures such as MSE are critical to integrative evaluation of living systems. When long-range coupling of systems breaks down, essential information exchange between them stops and this is associated with disease. Some diseases, such as neonatal Sepsis and Sepsis-like illnesses could be diagnosed using entropy before clinical signs appear and clinical diagnosis is made [8, 47, 50].

Caution must be taken when using MSE analysis not to focus on asymptotic and isolated values of entropy and specially in interpreting the process and output of different dynamical processes. In addition to specific measures of MSE, the dependence of these values on resolution, i.e., their scale should be considered for objective characterization of a physiologic event or process. MSE method quantifies the level of disorder at all relevant levels of resolution of the signal and that is why it offers a reliable measure of complexity [50, 53].

Fetal heart rate and heart rate variability are two of the most integrative sources of information for studying autonomic nervous system's development with gestational age. Neurodevelopment at every state is affected by the intertwined interaction of sympathetic and parasympathetic (vagal) systems. However, conventional methods and metrics of HR and HRV (discussed above) have not been able to understand and represent this interaction accurately or comprehensively [48].

With respect to fetal HRV, these single-scale measures have reported conflicting conclusions. For example, according to these complexity increases with increasing gestational age, and also decreases because of emerging patterns of heart rate acceleration as the fetus matures [48].

This has caused experts and researchers to move towards HRV indices which incorporate behavioral patterns and offer more information about developing of complex systems and maturation of autonomic control. Multiscale entropy is useful because it offers insights into Multiscale complexity throughout gestation.

In the growing fetus, short scale complexity increase throughout gestation is indicative of rising number of components involved in development. A simultaneous decrease in long scale complexity could signify the progressing synchronization and regularity of each component alone and in relationship with the rest of component [48]. Complexity is therefore linked to maturation, and increasing as well as decreasing as behavioral states are established.

### **Poincare Plot**

One commonly used nonlinear method that is simple to interpret is the Poincaré plot. It is a graphical representation of the correlation between successive RR intervals, i.e. plot of  $RR_{j+1}$  as a function of  $RR_j$  [35]. Also called a return map, this is a scatter plot drawn based on plotting each RR interval against the prior interval. It enables researchers to visually inspect and find patterns hidden in a sequence of RR intervals from successive measurements [49]. The shape of this plot has already been proven useful in assessing the degree of cardiac failure or dysfunction in adults [54].

The Poincare plot is drawn from nonlinear dynamics and is intended to demonstrate the fluctuations between RR intervals visually. Even though it is introduced and used as a nonlinear

method for HRV analysis, mathematically it has been proven that it correlates with standard time domain metrics extremely closely and via linear equations [54] .

SD1, a measure of the width of the ellipse and SD2, the measure of length of the plot are the two common descriptors of the Poincare plot. However [54] have proved that SD1 is really just the scaled version of the standard deviation of the successive intervals and therefore both SD1 and SD2 are related to the autocovariance function through a linear relationship. This demonstrates SD1 is extremely highly and linearly correlating with standard measures of HRV such as SDDSD index. In addition, SD2 relates highly and linearly to the standard traditional HRV measures of SDRR and SDDSD. One could say that SD2 is a measure of long term HRV because SDRR is used as a measure of long term variability. However that is not most accurate. SD2 is a measure of all the variability, both long-term and short-term [35, 54].

While the Poincare analysis's uses in demonstrating beat to beat dynamics of the heart should not be overlooked, current ways of interpreting this plot ignore this capacity and reduce its use to a simple statistical prop for highlighting traditional metrics. Still, there are some techniques through which this plot can give independent and truly nonlinear assessment of the heart and these are mostly working with number of peaks and the distance of them from the line of identity. The issue is these are not as dominant, well known or popular as the mainstream methods of interpreting Poincare plot [54] .

### **Stress Index And PNS/SNS Indexes**

#### *Baevsky's stress index*

Baevsky's stress index is calculated according to the following equation,

$$SI = \frac{AMo \times 100\%}{2Mo \times MxDMn}$$

Equation 14

In this equation, Mo is the most frequent RR interval (the mode) which is obtained as the median of RR interval. AMo is the amplitude of mode in percentage and is considered to be the height of the normalized RR interval histogram. MxDMn is the variation scope which represents the degree of RR interval variation. MxDMn is estimated as the difference of shortest and longest RR interval values. For decreasing sensitivity of the stress index value to slow changes in Mean HR, RR interval time series should be detrended using the smoothness priors method to eliminate the very low frequency trends [46].

#### *SNS Index*

There are several parameters that are used as the basis of calculating SNS index. With increased sympathetic activity the HR increases. Therefore, Mean HR (bpm) is an obvious choice for the SNS index equations. The stress index is widely applied as a measure of cardiovascular stress and therefore is the second parameter in calculation of SNS index. The third metric for estimating SNS index is SD2 from the Poincare plot [46]. When calculating SNS index, the square root of SI is taken for obtaining a normal distribution and also making the SNS index less vulnerable to extreme SI values.

#### *PNS Index*

Parasympathetic nervous system decreases HR and therefore increases the values of RR interval and its mean. Mean RR (ms) therefore is the first choice of input for calculating PNS index because it directly changes with parasympathetic regulation. Vagal activity influences the



magnitude of RSA, shown as quick and observable increases in RR interval with exhalation and quick decreases in RR interval values with exhalation. The RSA therefore is most correlated to RMSSD because it signifies quick beat-to-beat variations. Therefore, the second parameter that goes into calculation of PNS index is RMSSD. The third parameter for PNS index computation is SD1 from the Poincare plot which is closely related to RMSSD [46, 54] .

The parameters which are used as inputs for the calculation of SNS and PNS index, are first scaled with their standard deviations from their own normal population values. Then for reliable SNS and PNS index calculations a proprietary weighing is also used. An example of the comparison of PNS and SNS indexes with normal (resting) values from Kubios is shown in figure 9.

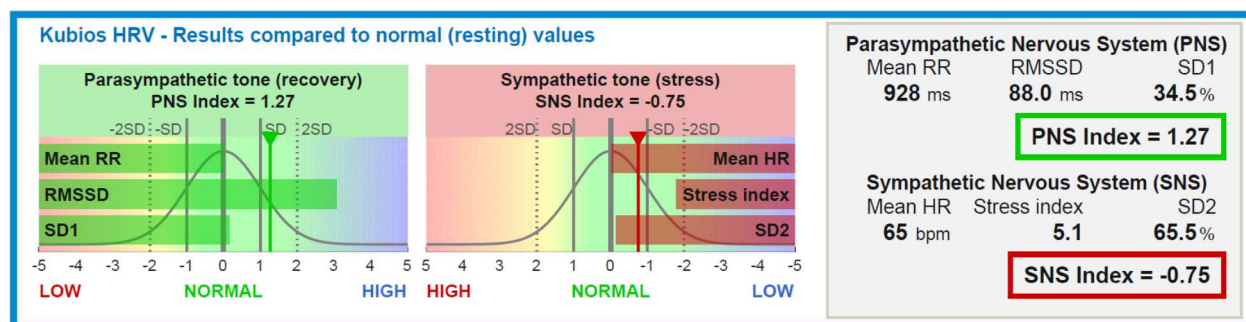


Figure 9. PNS and SNS index

## Chapter 4: Results

Table 1 shows the mean sample entropy for 43 fetal and 33 maternal subjects for 32- and 36-weeks gestational age. Average of sample entropy decreases from 32 to 36 weeks for the mother and increases for the fetus.

Table 6. Fetal and Maternal Average Sample Entropy

	32 weeks	36 weeks
Fetal	0.56784	0.662739
Maternal	1.192773	1.068124

Multiscale entropy, which is the focus of this thesis, is a non-standard and nonlinear HRV measure. Therefore, the first step to understand how MSE characterizes the autonomic development of the fetus, is to determine how MSE compares and contrasts between adults with parasympathetic dominance and the ones with sympathetic dominance. In order to do so, subject one, a mother with parasympathetic dominance, and subject two, with sympathetic dominance were selected for comparison. The initial assumptions about the autonomic control in these individuals were confirmed by the use of standardized time and frequency domain metrics. Subject 1 displays lower Mean HR, SNS index, Stress index and higher PNS index, SNDD, RMSSD, relative HF power, and entropy than subject 2. As shown in figures 10 and 11, the round vs. narrow distribution of Poincare plot respectively in subject 1 vs. 2 reflects more balance between short term and long term heart rate variability in subject 1.

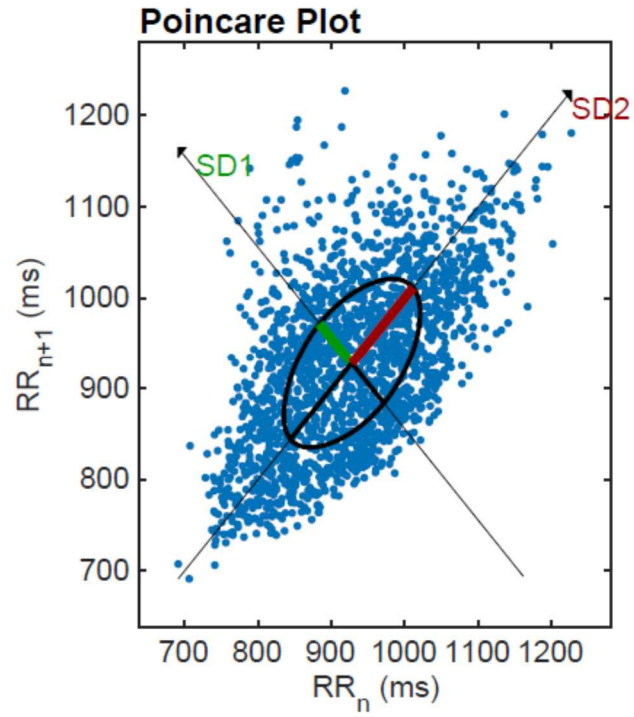


Figure 10. Poincare Plot - subject 1

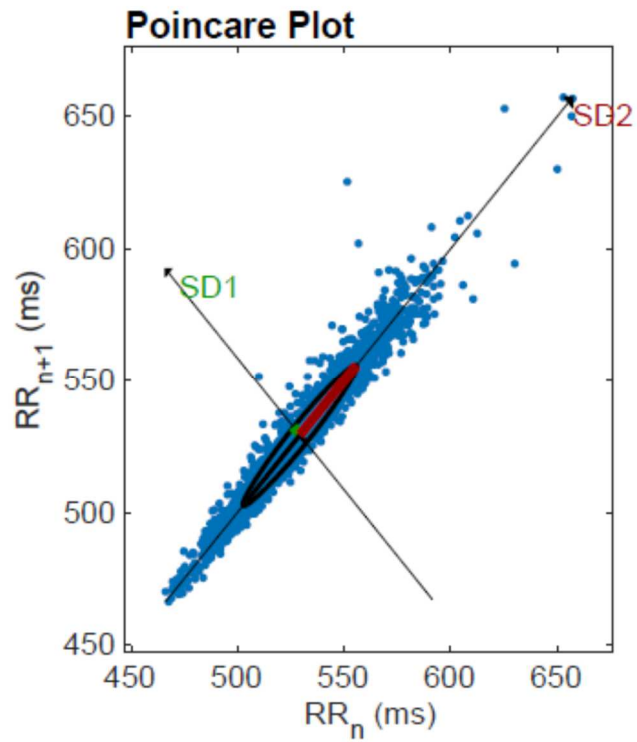


Figure 11. Poincare Plot, subject 2

Figure 12 shows the MSE for all 20 scales for subject one and subject two. As observed here, the short scale entropies for subject one are higher than subject two, but the long scale entropies in subject 2 are higher than subject 1. This shows smaller values at short scales of entropy correspond to higher SNS input and in contrast, smaller entropy values at long scales of entropy are associated with higher PNS control.

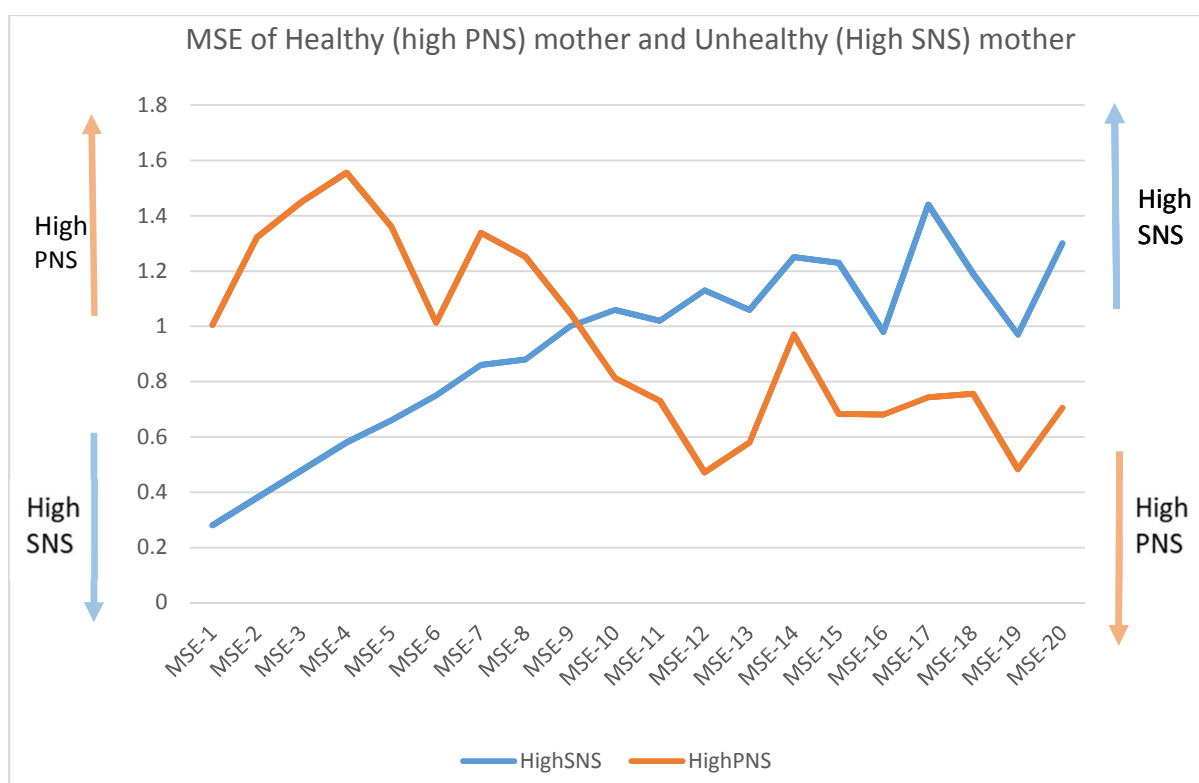


Figure 12. Scale 1 to 20 MSE for subject 1 (high PNS) and subject two (low PNS)

To further investigate this, after averaging the MSE of 142 other subjects for each scale, by performing the median split of MSE1 (which is the same as SampEn), the participants are divided into two groups of high versus low sample entropy. Figure 13 shows a similar pattern as observed

for the individuals in figure 12. The high entropy group has larger short scale entropies and smaller long scale entropies. Table 7 shows the means and standard deviations of both groups.

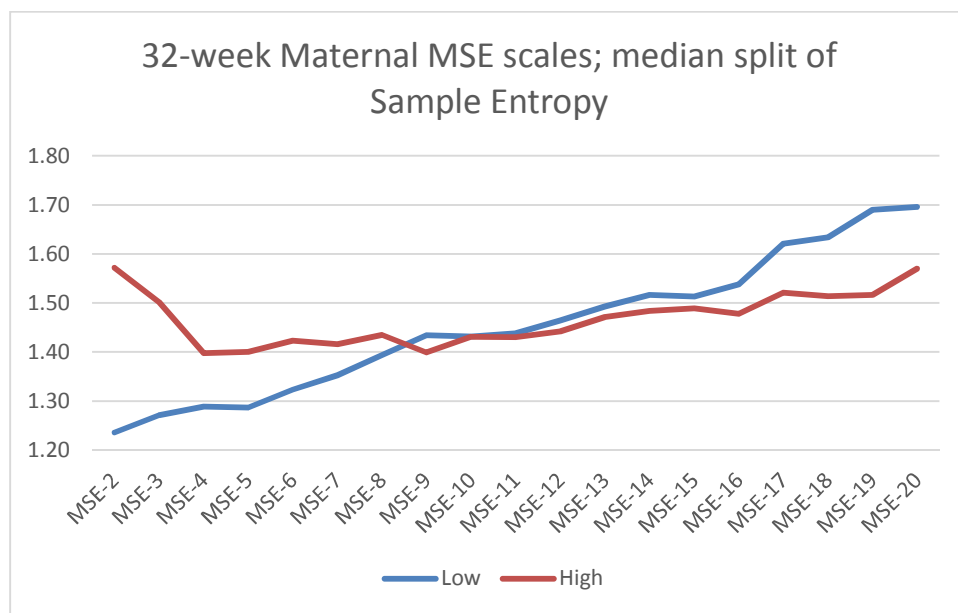


Figure 13. Median split of sample entropy (MSE 1) in two groups of 71 individuals each

Table 7. mean and SD of multiscale entropies of subjects in figure 13- The mean and SD MSE scales 2-20 of 142 pregnant women are shown in table 2. A median split of the 142 samples allowed the classification of two groups; low and high sample entropy.

	mse2	mse3	mse4	mse5	mse6	mse7	mse8	mse9	mse10	mse11	mse12	mse13	mse14	mse15	mse16	mse17	mse18	mse19	mse20
low	1.24 (0.30)	1.27 (0.28)	1.29 (0.27)	1.29 (0.27)	1.32 (0.27)	1.35 (0.28)	1.39 (0.30)	1.43 (0.30)	1.43 (0.30)	1.44 (0.27)	1.46 (0.28)	1.49 (0.33)	1.52 (0.34)	1.51 (0.32)	1.54 (0.34)	1.62 (0.38)	1.63 (0.38)	1.49 (0.41)	1.70 (0.42)
high	1.57 (0.16)	1.50 (0.16)	1.40 (0.15)	1.40 (0.14)	1.42 (0.16)	1.42 (0.16)	1.44 (0.17)	1.40 (0.17)	1.43 (0.22)	1.43 (0.19)	1.44 (0.20)	1.47 (0.22)	1.48 (0.25)	1.49 (0.27)	1.48 (0.27)	1.52 (0.33)	1.51 (0.33)	1.52 (0.34)	1.57 (0.40)

This gives us a profile for the behavior of the scales with respect to the dominance of sympathetic or parasympathetic control by the autonomic nervous system. Based on this

investigative practice to contrast the behavior of scales of entropy with high sympathetic and parasympathetic dominance, and knowing that vagal contribution in fetus increases in the final 8-10 weeks of gestation, we expect that MSE data of our 43 fetal subjects reflects increasing parasympathetic input as the fetus matures from 32 weeks to 36 weeks. Using the information gained from analyzing the maternal MSE scales and observing the influence of parasympathetic and sympathetic input on short and long scales, we would predict that MSE scales 1-5 would increase between 32 and 36 weeks gestational age and MSE scales 15-20 would decrease between 32 and 36 weeks gestational age. Figure 14, the Multiscale entropies of the 43 fetal subjects, confirms this expectation. For scales 1-5, 36 weeks MSE values are higher than 32 weeks MSE values. Also for scales 14 and higher, 36 weeks MSE values are lower than 32 weeks.

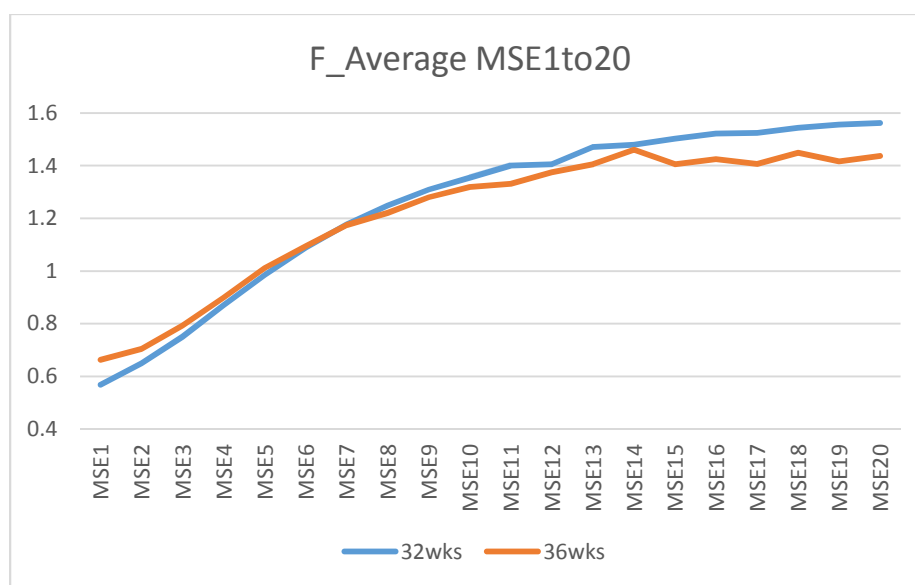


Figure 14. Scale 1 to 20 average MSE for 43 fetal subjects - 32 wks and 36 wks

Figure 15 shows an increase in the average Multiscale entropies of 33 pregnant women across all scales. With advancing gestation, an overall reduction in complexity is observed. However this is in contrast with Figure 14, in which fetal MSE scales reflect the effect of maturation and increasing parasympathetic influence.

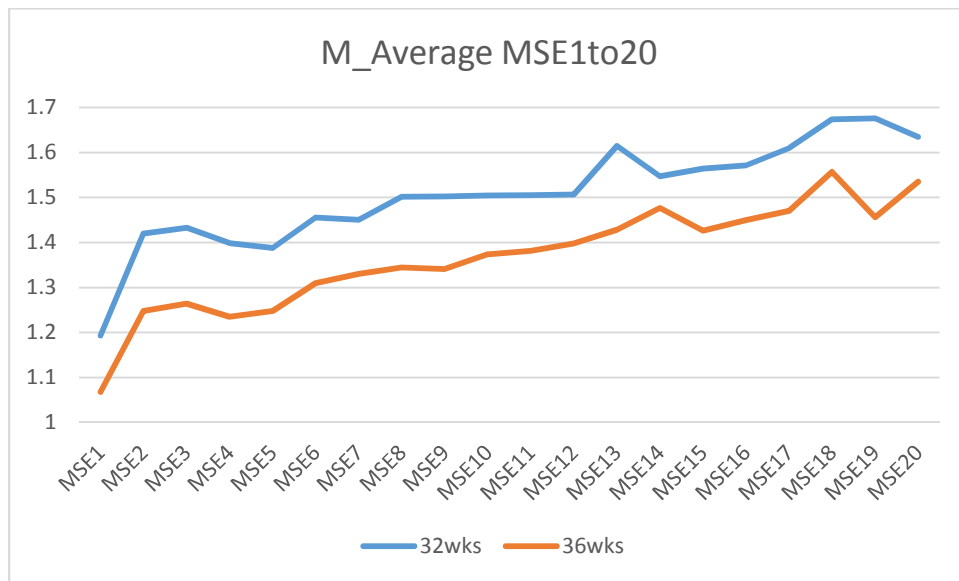


Figure 15. Scale 1 to 20 average MSE for 33 maternal subjects - 32 wks and 36 wks

## Chapter 5: Discussion

The first aim of this work was learning about the autonomic nervous system of the developing fetus and the physiology of pregnancy, analysis of heart rate variability, pros and cons of standard and traditional HRV metrics, and how to apply nonlinear methodologies to the fetus, currently practiced by very few researchers in the field.

Through attending and participating PANDA (Prenatal Autonomic Neuro-Developmental Assessment) clinical trial maternal and fetal visits during the first year of my graduate studies, I observed and learned the complete process of obtaining HRV data. With several trainings I received from Dr. Gustafson and her team, I learned about the principles of the biomagnetometer and its operation and maintenance. Through hands on work, I learned about the advantages and limitations of this machine and its use in multiple areas of research such as neuroscience, physiology, and psychology. I got familiar with EEGLAB as the next phase of analysis once the recording is obtained via the biomagnetometer. I analyzed several datasets obtained from previous and current studies. Then I practiced and interpreted the output of my EEGLAB analysis and understood how I can use the traditional and standard HRV metrics to determine the physiological meaning of fetal and maternal HRV data.

I also joined the recruiting team of ADORE (Assessment of DHA On Reducing Early preterm birth) and PANDA clinical trials to recruit participants in clinic and through this experience I realized the clinical implications of HR and HRV and became familiar with maternal and fetal conditions which interfere with or limit the application of HRV data towards research, conditions such as congenital heart defects or neural tube issues that with the use of biomagnetometer, could be studied and characterized on their own.



The second and central purpose of this thesis was to explore the value and capability of MSE in characterizing fetal maturation. Based on observations in figure 1 and 2, and the knowledge that parasympathetic influence increases with increasing gestational age, it was expected that at 36 weeks gestational age, scale ~1-5 MSEs would be higher than those at 32 weeks. Also, the MSE values for scales of ~15-20 were anticipated to be lower at 36 weeks than those at 32 weeks. This in fact is confirmed in Figure 4 which fetal Multiscale entropy trends of 43 fetal subjects. For scales 1-5, 36 weeks MSE values are higher than 32 weeks MSE values. Also for scales 14 and higher, 36 weeks MSE values are lower than 32 weeks.

This is consistent with results of a study of indices of maturing fetal autonomic control by Hoyer and colleagues [48] who found an increase in MSE based age related complexity in scales 1-9 and a decrease in MSE in scales of 15 and higher with advancing gestational age. Even though the analysis was done separately on groups of quiet and active states, similar observations were made in both groups [48]

For the fetus, Multiscale entropy reflects growth and increase in complexity by showing the effects of maturation on each and every scale individually. Together, the trends of 20 scales, specifically the first five and the last five scales from 32 to 36 weeks gestational age, show the increasing parasympathetic influence. Even though the fetus is under dominant control of the SNS, around 30-32 weeks gestation autonomic differentiation initiates parasympathetic processes and drives their development as the fetus grows. Therefore, parasympathetic regulation further advances [8]. This increase in parasympathetic input and autonomic nervous system development continues in the final 8-10 weeks of gestation until birth.

For understanding the capability of MSE in reflecting different systems, we examined maternal MSE scales between 32 and 36 weeks, and the results are shown in figure 4. These results

show MSE decreases across all scales with advancing pregnancy. Entropy changes of all the scales show the effect of increasing allostatic load accompanied by increase in physiologic stress and dampening of complexity. Maternal MSE trends show the linear effect of load exerted on the mother via pregnancy. This is expected because the physiological changes in maternal body to adapt to an increasing physiological load during pregnancy is associated with a decrease in entropy. Specifically increasing metabolic stress and circulatory capacity to handle additional blood flow are two of the most significant changes in the body of a pregnant woman [55]. Unlike ANS of the fetus, maternal ANS is fully developed, therefore there is no sign of maturation, growth and development in MSE scale trends. On the other hand the fetus is developing and the nonlinear influence of developing and growing ANS is reflected in the behavior of MSE scales.

This differs from the fetus, because the maternal ANS is already developed, and confirms the increasing allostatic load that results in a linear increase in physiologic stress and therefore dampening of complexity. Therefore, MSE can show interaction between developing organs in a growing system and linear effect of physiological load in a system which has already fully developed. In other words, MSE recognizes maturation related complexity change where there is one.

Based on this study, MSE has value in showing nonlinear complexity changes, characterizing the increasing interaction of the parasympathetic nervous system on autonomic control of the fetus during maturation. And when maturation and growth is absent, such as in maternal system, it shows the linear effect of factors such as allostatic load.

Based on its capability to recognize and measure complexity, Multiscale entropy can convey information about the ability of an organism to adapt to difficult situations such as difficult labor

and delivery, secondary illnesses, premature birth, etc. An organism with a more complex signal is more flexible and more likely to survive in a hostile environment.

There are surrogates for complexity but they are not universally adaptable. Greater entropy does not always signify more complexity and growth. Single scale entropies such as approximate entropy cannot distinguish between circumstances of chaos due to pathologies and maturation as the cause for increased complexity. The advantage and importance of Multiscale entropy is due to the fact that it retains the information overlooked by conventional measures because it captures dynamic characteristics displayed by these systems on multiple spatial and temporal scales [50]. We expect to see increasing complexity in a developing organism. With increased parasympathetic input and integration of the peripheral and central nervous systems we should observe definite neurobehavioral states in the fetus, heart rate patterns linked to fetal state and organization of movements. This constant and overall increase in complexity has been realized with the use of metrics such as mean RR interval, and its standard deviation, and root mean square of successive differences, but here we see that the MSE scales add a nonlinear metric that seems to accurately reflect the ontological development of the fetus [13].

## References

- [1] D. J. Barker, "The fetal and infant origins of adult disease," *BMJ*, vol. 301, p. 1111, Nov 17 1990.
- [2] D. J. Barker, "In utero programming of chronic disease," *Clin Sci (Lond)*, vol. 95, pp. 115-28, Aug 1998.
- [3] K. L. Grove, B. E. Grayson, M. M. Glavas, X. Q. Xiao, and M. S. Smith, "Development of metabolic systems," *Physiol Behav*, vol. 86, pp. 646-60, Dec 15 2005.
- [4] S. C. Langley-Evans, "Fetal programming of cardiovascular function through exposure to maternal undernutrition," *Proc Nutr Soc*, vol. 60, pp. 505-13, Nov 2001.
- [5] J. A. Armitage, L. Poston, and P. D. Taylor, "Developmental origins of obesity and the metabolic syndrome: The role of maternal obesity," *Obesity and Metabolism*, vol. 36, pp. 73-84, 2008.
- [6] C. Vasudevan, M. Renfrew, and W. McGuire, "Fetal and perinatal consequences of maternal obesity," *Arch Dis Child Fetal Neonatal Ed*, vol. 96, pp. F378-82, Sep 2011.
- [7] E. A. P. Kathleen M. Gustafson, "Fetal Assessment Using Biomagnetometry: Neurobehaviors, Cardiac Autonomic Control, and Research Applications," in *Fetal Development - Research on Brain and Behavior, Environmental Influences, and Emerging Technologies*, B. S. K. Nadja Reissland, Ed., ed, 2016.
- [8] J. A. DiPietro, K. A. Costigan, and K. M. Voegtline, "Studies in Fetal Behavior: Revisited, Renewed, and Reimagined," *Monogr Soc Res Child Dev*, vol. 80, pp. vii;1-94, Sep 2015.
- [9] J. G. Nijhuis, H. F. Prechtl, C. B. Martin, Jr., and R. S. Bots, "Are there behavioural states in the human fetus?," *Early Hum Dev*, vol. 6, pp. 177-95, Apr 1982.
- [10] I. J. Nijhuis and J. ten Hof, "Development of fetal heart rate and behavior: indirect measures to assess the fetal nervous system," *Eur J Obstet Gynecol Reprod Biol*, vol. 87, pp. 1-2, Nov 1999.
- [11] J. A. DiPietro, S. C. Hilton, M. Hawkins, K. A. Costigan, and E. K. Pressman, "Maternal stress and affect influence fetal neurobehavioral development," *Dev Psychol*, vol. 38, pp. 659-68, Sep 2002.
- [12] J. A. DiPietro, K. A. Costigan, E. K. Pressman, and J. A. Doussard-Roosevelt, "Antenatal origins of individual differences in heart rate," *Dev Psychobiol*, vol. 37, pp. 221-8, Dec 2000.
- [13] P. Van Leeuwen, S. Lange, H. Bettermann, D. Gronemeyer, and W. Hatzmann, "Fetal heart rate variability and complexity in the course of pregnancy," *Early Hum Dev*, vol. 54, pp. 259-69, Apr 1999.
- [14] M. David, M. Hirsch, J. Karin, E. Toledo, and S. Akselrod, "An estimate of fetal autonomic state by time-frequency analysis of fetal heart rate variability," *J Appl Physiol*, vol. 102, pp. 1057-64, Mar 2007.
- [15] R. Tao, "Advanced Source Reconstruction and Volume Conductor Modeling for Fetal Magnetocardiography," Ph.D., Bioengineering, University of Kansas, 2015.
- [16] R. T. Wakai, "Assessment of fetal neurodevelopment via fetal magnetocardiography," *Exp Neurol*, vol. 190 Suppl 1, pp. S65-71, Nov 2004.
- [17] H. Zhao and R. T. Wakai, "Simultaneity of foetal heart rate acceleration and foetal trunk movement determined by foetal magnetocardiogram actocardiography," *Phys Med Biol*, vol. 47, pp. 839-46, Mar 7 2002.

- [18] P. Van Leeuwen, D. Geue, S. Lange, D. Cysarz, H. Bettermann, and D. H. Gronemeyer, "Is there evidence of fetal-maternal heart rate synchronization?," *BMC Physiol*, vol. 3, p. 2, Apr 17 2003.
- [19] P. Van Leeuwen, D. Geue, M. Thiel, D. Cysarz, S. Lange, M. C. Romano, *et al.*, "Influence of paced maternal breathing on fetal-maternal heart rate coordination," *Proc Natl Acad Sci U S A*, vol. 106, pp. 13661-6, Aug 18 2009.
- [20] P. Ivanov, Q. D. Ma, and R. P. Bartsch, "Maternal-fetal heartbeat phase synchronization," *Proc Natl Acad Sci U S A*, vol. 106, pp. 13641-2, Aug 18 2009.
- [21] D. Hoyer, F. Tetschke, S. Jaekel, S. Nowack, O. W. Witte, E. Schleussner, *et al.*, "Fetal functional brain age assessed from universal developmental indices obtained from neuro-vegetative activity patterns," *PloS one*, vol. 8, p. e74431, 2013.
- [22] E. A. Popescu, M. Popescu, T. L. Bennett, J. D. Lewine, W. B. Drake, and K. M. Gustafson, "Magnetographic assessment of fetal hiccups and their effect on fetal heart rhythm," *Physiol Meas*, vol. 28, pp. 665-76, Jun 2007.
- [23] E. A. Popescu, M. Popescu, J. Wang, S. M. Barlow, and K. M. Gustafson, "Non-nutritive sucking recorded in utero via fetal magnetography," *Physiol Meas*, vol. 29, pp. 127-39, Jan 2008.
- [24] K. M. Gustafson, J. J. Allen, H. W. Yeh, and L. E. May, "Characterization of the fetal diaphragmatic magnetomyogram and the effect of breathing movements on cardiac metrics of rate and variability," *Early Hum Dev*, Apr 13 2011.
- [25] L. E. May, A. Glaros, H. W. Yeh, J. F. Clapp, 3rd, and K. M. Gustafson, "Aerobic exercise during pregnancy influences fetal cardiac autonomic control of heart rate and heart rate variability," *Early Hum Dev*, vol. 86, pp. 213-7, Apr 2010.
- [26] L. E. May, R. R. Suminski, A. Berry, M. D. Langaker, and K. M. Gustafson, "Maternal physical activity mode and fetal heart outcome," *Early Hum Dev*, vol. 90, pp. 365-9, Jul 2014.
- [27] K. M. Gustafson, J. Colombo, and S. E. Carlson, "Docosahexaenoic acid and cognitive function: Is the link mediated by the autonomic nervous system?," *Prostaglandins Leukot Essent Fatty Acids*, vol. 79, pp. 135-40, Sep-Nov 2008.
- [28] K. M. Gustafson, S. E. Carlson, J. Colombo, H. W. Yeh, D. J. Shaddy, S. Li, *et al.*, "Effects of docosahexaenoic acid supplementation during pregnancy on fetal heart rate and variability: a randomized clinical trial," *Prostaglandins, leukotrienes, and essential fatty acids*, vol. 88, pp. 331-8, May 2013.
- [29] S. W. Porges, "Cardiac vagal tone: a physiological index of stress," *Neurosci Biobehav Rev*, vol. 19, pp. 225-33, Summer 1995.
- [30] P. K. Stein, M. T. Hagley, P. L. Cole, P. P. Domitrovich, R. E. Kleiger, and J. N. Rottman, "Changes in 24-hour heart rate variability during normal pregnancy," *Am J Obstet Gynecol*, vol. 180, pp. 978-85, Apr 1999.
- [31] J. S. Richman and J. R. Moorman, "Physiological time-series analysis using approximate entropy and sample entropy," *Am J Physiol Heart Circ Physiol*, vol. 278, pp. H2039-49, Jun 2000.
- [32] A. Delorme and S. Makeig, "EEGLAB: an open source toolbox for analysis of single-trial EEG dynamics including independent component analysis," *J Neurosci Methods*, vol. 134, pp. 9-21, Mar 15 2004.
- [33] L. D. Devoe, "Nonstress testing and contraction stress testing," *Obstet Gynecol Clin North Am*, vol. 26, pp. 535-56, v, Dec 1999.

- [34] A. Piontelli, *Development of normal fetal movements : the first 25 weeks of gestation*. Milan: Springer, 2010.
- [35] J. L. Mika P. Tarvainen, Juha-Pekka Niskanen, Perttu O. Ranta-aho, "Kubios HRV User's Guide," K. Oy, Ed., ed, 2018.
- [36] V. Kariniemi, J. Ahopelto, P. J. Karp, and T. E. Katila, "The fetal magnetocardiogram," *J Perinat Med*, vol. 2, pp. 214-6, 1974.
- [37] Z. Li, J. F. Strasburger, B. F. Cuneo, N. L. Gotteiner, and R. T. Wakai, "Giant fetal magnetocardiogram P waves in congenital atrioventricular block: a marker of cardiovascular compensation?," *Circulation*, vol. 110, pp. 2097-101, Oct 12 2004.
- [38] S. Lange, P. Van Leeuwen, U. Schneider, B. Frank, D. Hoyer, D. Geue, *et al.*, "Heart rate features in fetal behavioural states," *Early Hum Dev*, vol. 85, pp. 131-5, Feb 2009.
- [39] R. P. Bartsch, K. K. Liu, A. Bashan, and P. Ivanov, "Network Physiology: How Organ Systems Dynamically Interact," *PLoS One*, vol. 10, p. e0142143, 2015.
- [40] T. Menendez, S. Achenbach, E. Beinder, M. Hofbeck, L. Klinghammer, H. Singer, *et al.*, "Usefulness of magnetocardiography for the investigation of fetal arrhythmias," *Am J Cardiol*, vol. 88, pp. 334-6, Aug 1 2001.
- [41] A. delorme, t. Fernsler, H. Serby, and S. Makeig, "EEGLAB tutorial," U. o. S. D. California, Ed., ed, 2006.
- [42] A. J. Bell and T. J. Sejnowski, "An information-maximization approach to blind separation and blind deconvolution," *Neural Comput*, vol. 7, pp. 1129-59, Nov 1995.
- [43] S. Amari, A. Cichocki, and H. H. Yang, "A New Learning Algorithm for Blind Signal Separation," in *Advances in Neural Information Processing Systems 8*, ed Cambridge: MIT Press, 1996, pp. 757-763.
- [44] C. J. James and C. W. Hesse, "Independent component analysis for biomedical signals," *Physiol Meas*, vol. 26, pp. R15-39, Feb 2005.
- [45] D. Mantini, K. E. Hild, 2nd, G. Alleva, and S. Comani, "Performance comparison of independent component analysis algorithms for fetal cardiac signal reconstruction: a study on synthetic fMCG data," *Phys Med Biol*, vol. 51, pp. 1033-46, Feb 21 2006.
- [46] K. OY, "About Heart Rate Variability," K. OY, Ed., ed, 2019.
- [47] D. E. Lake, J. S. Richman, M. P. Griffin, and J. R. Moorman, "Sample entropy analysis of neonatal heart rate variability," *American journal of physiology. Regulatory, integrative and comparative physiology*, vol. 283, pp. R789-97, Sep 2002.
- [48] D. Hoyer, S. Nowack, S. Bauer, F. Tetschke, A. Rudolph, U. Wallwitz, *et al.*, "Fetal development of complex autonomic control evaluated from multiscale heart rate patterns," *Am J Physiol Regul Integr Comp Physiol*, vol. 304, pp. R383-92, Mar 1 2013.
- [49] F. Shaffer and J. P. Ginsberg, "An Overview of Heart Rate Variability Metrics and Norms," *Front Public Health*, vol. 5, p. 258, 2017.
- [50] M. Costa, A. L. Goldberger, and C. K. Peng, "Multiscale entropy analysis of complex physiologic time series," *Phys Rev Lett*, vol. 89, p. 068102, Aug 5 2002.
- [51] G. P. P. I., "Estimation of the Kolmogorov entropy from a chaotic signal," *PHYSICAL REVIEW A*, vol. 28, 1983.
- [52] P. WenbinShi, YanMa, ShuchenSun, Chien-HungYeh, "A comparison study on stages of sleep: Quantifying multiscale complexity using higher moments on coarse-graining," *Elsevier*, vol. 44, pp. 292-303, 2017.

- [53] M. D. Costa and A. L. Goldberger, "Generalized Multiscale Entropy Analysis: Application to Quantifying the Complex Volatility of Human Heartbeat Time Series," *Entropy (Basel)*, vol. 17, pp. 1197-1203, Mar 2015.
- [54] M. Brennan, M. Palaniswami, and P. Kamen, "Do existing measures of Poincare plot geometry reflect nonlinear features of heart rate variability?," *IEEE Trans Biomed Eng*, vol. 48, pp. 1342-7, Nov 2001.
- [55] M. Baumert, M. Javorka, A. Seeck, R. Faber, P. Sanders, and A. Voss, "Multiscale entropy and detrended fluctuation analysis of QT interval and heart rate variability during normal pregnancy," *Comput Biol Med*, vol. 42, pp. 347-52, Mar 2012.